

DEPARTMENT OF MINES AND ENERGY  
GEOLOGICAL SURVEY  
SOUTH AUSTRALIA



REPORT BOOK NO. 92/2

GEOPHYSICAL APPRAISAL OF  
NORTHERN KANGAROO ISLAND

B J VAN DER STELT

A P BELPERIO

and

R B FLINT

Regional Geology

JANUARY 1992

DME 425/89

©Department of Mines and Energy South Australia 1992.  
This report is subject to copyright. Apart from fair dealing for the purposes of study, research, criticism or review,  
as permitted under the Copyright Act, no part may be reproduced without written permission  
of the Director-General, Department of Mines and Energy South Australia.

<u>CONTENTS</u>	<u>PAGE</u>
ABSTRACT	1
INTRODUCTION	1
REGIONAL GEOLOGY	1
REGIONAL GEOPHYSICS	3
GEOPHYSICAL APPRAISAL	3
Magnetic Susceptibility	3
Survey Information	4
Modelling	4
Aeromagnetic Line 240	4
Aeromagnetic Line 210	5
Aeromagnetic Line 176/171	5
Aeromagnetic Line 9170	5
Aeromagnetic Line 9141	6
Aeromagnetic Line 9120	6
Aeromagnetic Line 9122	7
Gravity Line 3A	7
Gravity Line 2A	8
SUMMARY	8
REFERENCES	10

<u>FIGURES</u>	<u>Plan No</u>
1. Tectonic provinces associated with the southern Gawler Craton margin.	S22438
2. Regional geology and location plan of geophysical surveys.	91-464
3. Bouguer gravity contours (milligals) for Kangaroo Island, Yorke Peninsula and Gulf St Vincent area.	S22439
4. Total magnetic intensity contours for the Kangaroo Island region. Combination of 1982 Geoex Pty Ltd and 1957 BMR Surveys.	91-465
5. Aeromagnetic profile, model and geological interpretation, Line 240.	91-466

6.	Aeromagnetic profile, model and geological interpretation, Line 210.	91-467
7.	Aeromagnetic profile, model and geological interpretation, Line 176/171.	91-468
8.	Aeromagnetic profile, model and geological interpretation, Line 9170.	91-469
9.	Aeromagnetic profile, model A and geological interpretation, Line 9141.	91-470
10.	Aeromagnetic profile, model B and geological interpretation, Line 9141.	91-471
11.	Aeromagnetic profile, model and geological interpretation, Line 9120.	91-472
12.	Aeromagnetic profile, model and geological interpretation, Line 9122.	91-473
13.	Gravity profile, model and geological interpretation, Line 3A.	91-474
14.	Enlargement of gravity model and geological interpretation, Line 3A.	91-475
15.	Gravity profile, model and geological interpretation, Line 2A.	91-476
16.	Tectonic map and synthesis of depth to magnetic basement (Lincoln Complex)	91-477.

APPENDIX A - Magnetic susceptibilities for various rock units.

APPENDIX B - Data Diskette.

## Geophysical Appraisal of Northern Kangaroo Island

B J VAN DER STELT  
A P BELPERIO and  
R B FLINT

**Crystalline basement of the Gawler Craton continues further southwards than previously interpreted, extending under northern Kangaroo Island. Depths to basement range from 200m near Emu Bay, ~250-750m inland from Cape Cassini to greater depths elsewhere. Basement, assumed to be Palaeoproterozoic Lincoln Complex, is terminated by a complex fault zone analogous in character to the Torrens Hinge Zone of the eastern Gawler Craton.**

### INTRODUCTION

Revision of the regional geology of the KINGSCOTE 1:250 000 geological map sheet area incorporates delineation of the southern margin of the Gawler Craton. Traditionally as shown by Flint and Parker (1982), the Gawler Craton's margin has been located within Investigator Strait (Fig. 1). However, a recent reappraisal based on shallow offshore seismic and dredging (Mineral Industry Quarterly, 57) indicates the boundary may be further south than previously considered, to the extent that it may underlie northern Kangaroo Island. This area was selected for geophysical investigation - including computer modelling of existing aeromagnetic data, additional ground magnetic traverses and two gravity profiles. Estimated depths to Palaeoproterozoic crystalline basement have been modelled, to enable potential sites to be selected for stratigraphic drilling to appraise the cover sequences and nature of the underlying basement.

In the computer modelling, the models selected are

not the only possible solutions as parameters like depth and density are variable and interdependent. Different combinations of parameters can produce similar theoretical profiles. Recent unpublished geological mapping data were used along with magnetic susceptibility measurements to produce observed versus theoretical profiles and associated geological interpretations.

### REGIONAL GEOLOGY

Crystalline basement rocks of the Gawler Craton are exposed on southern Yorke Peninsula and on various islands in Investigator Strait and southern Spencer Gulf. The basement is part of the Palaeoproterozoic Donington Granitoid Suite of the Lincoln Complex and consists predominantly of orthogneisses, including deformed megacrystic granite, charnockite, granodiorite, leucogranite and aplite.

Rb-Sr geochronology on various units within the Donington Granitoid Suite has produced ages of 1794

$\pm 40$  Ma (Webb *et al.*, 1986) and  $1818 \pm 13$  Ma (Mortimer *et al.*, 1979). However, these ages reflect metamorphic episodes, as the emplacement age, as deduced from U-Pb zircon analysis, is  $1843 \pm 2$  Ma (Mortimer *et al.*, 1986).

Intruding the Donington Granitoid Suite are numerous metadolerite dykes forming a dyke swarm subparallel to the regional foliation. Principal lithologies are norite, gabbro and dolerite, and their intrusive age(s) may be as young as 1600 Ma (Mortimer *et al.*, 1988).

No exposures of Lincoln Complex crystalline basement occur on Kangaroo Island, with the nearest known occurrences being in Investigator Strait on Orcades Bank and two knolls northeast of Cape Borda (Rankin *et al.*, 1991).

The oldest units on Kangaroo Island are Neoproterozoic strata of the Adelaide Geosyncline exposed in the core of a major regional anticline on Dudley Peninsula; sediments include representatives of the Umberatana and Normanville Groups (Daily *et al.*, 1979). Their distribution elsewhere on the island is not known for they are concealed by younger Cambrian sediments of the Stansbury Basin and Kanmantoo Trough.

North of the Cygnet and Snelling Faults, sediments of the Stansbury Basin are predominantly shelf clastics and carbonates (Fig. 2). Units in ascending stratigraphic sequence are Mt McDonnell Formation, Stokes Bay Sandstone, Smith Bay Shale, White Point Conglomerate, Emu Bay Shale and Boxing Bay Formation. The sequence has been mildly deformed with broad open folds and low greenschist facies

metamorphism.

South of the Cygnet and Snelling Faults, Cambrian sediments are all part of the Kanmantoo Trough and represent deposition in outer shelf - deeper water environments. Metamorphic grade is higher at upper greenschist to locally mid-amphibolite facies, deformation more intense, and there are numerous granite intrusives, migmatites and pegmatite dykes. These events resulted from the Delamerian Orogeny of Late Cambrian-Ordovician age.

During the Carboniferous-Permian, southern Australia was very close to the southern rotational axis and experienced glaciation. Large glaciers flowed northwestwards, deeply eroding the underlying Cambrian strata. Remnants of till and glacial striae are well preserved on eastern Kangaroo Island.

Separation and breakup of Gondwana was initiated in the Jurassic. Rifting between Antarctica and Australia is reflected on Kangaroo Island by outpouring of tholeiitic basalt lava, now preserved as a thin sheet west of Kingscote, and an isolated remnant on Dudley Peninsula.

Tertiary sediments on Kangaroo Island are thin but widespread, with remnants of marine sediments of Eocene, Oligocene, Miocene and Pliocene age. Weathering profiles, especially laterite, are common and, along with the Quaternary record, are summarised in Daily *et al.* (1979).

## REGIONAL GEOPHYSICS

The Bouguer anomaly gravity map for the region (Fig. 3) shows a broad northwest-trending regional high of +30 milligals over central Investigator Strait and extending onto northern Kangaroo Island in the vicinity of Cape Cassini. Other broad regional highs are coincident with exposures of Lincoln Complex crystalline basement on Yorke Peninsula and southern Eyre Peninsula. The presence of knolls within Investigator Strait consisting of Lincoln Complex granitoids implies that the regional gravity high reflects shallow basement.

A northeast-trending gravity high (+20 milligals) on Dudley Peninsula broadly corresponds to a major anticline, in the core of which are exposed Adelaidean sediments. The gravity response is probably due to crystalline basement at depth.

The total magnetic intensity map (Fig. 4) supports the interpretation of the gravity data. The central Investigator Strait region consists of numerous, small, discrete anomalies which collectively define a northwest-trending zone of high-amplitude anomalies extending onto Yorke Peninsula. The pattern, consistent with shallow crystalline basement, extends southeastwards to the northern coastline of Kangaroo Island. Anomalies continue inland from Cape Cassini but are broader, suggesting continuation of the crystalline basement but at a greater depth. A very large and broad aeromagnetic high near Kingscote also probably reflects deep crystalline basement.

The aeromagnetic highs near Kingscote and inland from Cape Cassini and also the regional gravity high for northern Kangaroo Island all have steep gradients on their southern margins suggestive of major east-west faulting. This is reflected on the surface by the Cygnet and Snelling Faults. South of the fault zone and applicable for most of Kangaroo Island, the aeromagnetic characteristics suggest a thick sedimentary sequence and very deep crystalline basement.

## GEOPHYSICAL APPRAISAL

### Magnetic Susceptibility

Before computer modelling commenced, magnetic susceptibilities were measured on hand specimens from various Phanerozoic and Proterozoic units. The samples (collected by A.P.B. and R.B.F. during remapping of the KINGSCOTE 1:250 000 map sheet) are currently stored at the Department of Mines and Energy Core Library, Glenside. The measurements, in SI units, were taken with a hand held susceptibility meter. These figures were converted to cgs units by dividing by a factor of  $4\pi$  for compatibility with the Toolkit modelling program. A full listing of the rock sample (R.S.) numbers, magnetic susceptibilities and rock types is given in Appendix A.

Most of the Phanerozoic rocks have very low magnetic responses, generally less than  $5 \times 10^{-5}$  cgs units, and were generally ignored in the magnetic modelling process. Rocks of these ages with higher susceptibilities include Jurassic basalts (up to  $39 \times 10^{-5}$

<sup>5</sup> cgs units). The most magnetic Phanerozoic unit is the Middleton Sandstone which contains heavy mineral-rich beds up to 1m thick resulting in magnetic susceptibilities up to  $250 \times 10^{-5}$  cgs units. These values are comparable to those for mafic granulites of the crystalline basement. However, occurrences of Middleton Sandstone are not known on northern Kangaroo Island and therefore it is considered that confusion between the two is unlikely.

Crystalline basement lithologies of the Gawler Craton have much higher magnetic susceptibilities. The granites average  $84 \times 10^{-5}$ , granulites  $105 \times 10^{-5}$ , gneisses  $60 \times 10^{-5}$ , dolerites  $49 \times 10^{-5}$ , and amphibolites  $69 \times 10^{-5}$  cgs units. However, each rock type shows great variation; gneisses for example range from as little as  $2 \times 10^{-5}$ , whereas granulites range as high as  $334 \times 10^{-5}$  cgs units. With this variability in mind, a range of  $40\text{-}170 \times 10^{-5}$  cgs units was adopted for the crystalline basement although attempts were made to restrict values to  $80\text{-}120 \times 10^{-5}$  cgs units.

## Survey Information

Aeromagnetic flight lines passing over magnetic highs near Hummocky Point-Cape Cassini, Cape D'Estaing and Emu Bay were selected for computer modelling (Fig. 2). Five lines selected from the 1982 South Stansbury Basin Aeromagnetic Survey are orientated east-west (lines 240 and 210) or north-south (lines 9170, 9141 and 9120). Two additional aeromagnetic lines from the 1982 survey (176/171 and 9122) and a ground gravity line (line 3A) were chosen to model the structure of the basement. A ground gravity line

(line 2A) was also chosen at American River in a region of minimal bedrock exposure. Copies of data files are stored on the MS-DOS compatible diskette in Appendix B.

The 1982 South Stansbury Basin Aeromagnetic Survey was flown at a nominal terrain clearance of 150m, sampling interval of 56m, and a flight-line spacing of 1000m.

## Modelling

Two-dimensional modelling was undertaken using the magnetic- and gravity-modelling software 'TOOLKIT' version 3. A total magnetic field strength of 60500 gammas and a magnetic field inclination of  $-67.5^\circ$  were used for northern Kangaroo Island. Modelled bodies are assumed by the program to strike perpendicularly to the geophysical profile. All magnetic modelled depths in Figs. 5-15 are given as depths below the flight lines which have a terrain clearance of  $\sim 150\text{m}$ . In the text, depths have been corrected and referenced to ground surface. All gravity-modelled depths are referenced to the ground surface. Magnetic susceptibilities are shown on each figure for the selected polygons. Where polygons are superimposed, their susceptibilities are summed.

### Aeromagnetic Line 240

A portion of this east-west trending line in the Emu Bay-Point Marsden area was selected to model an aeromagnetic high that impinges onto the north coast. The basement was assumed to be magnetically homogeneous over the distance of  $\sim 8$  km with a

susceptibility of  $130 \times 10^{-5}$  cgs units.

The model fit (Fig. 5) depicts a section of moderately shallow basement at the western end of the line (depths range from 600 to 850m below ground level) shallowing to a depth of ~210m at Bald Rock precisely below the magnetic maximum. Eastwards, the depths increase dramatically, possibly due to faulting, reaching 2500 m at the easternmost part of the section.

### **Aeromagnetic Line 210**

This east-west orientated line was chosen for its transect of a broad aeromagnetic high south of Cape Cassini. The data display a simple bell-shaped curve so only the portion of the line which covered the magnetic high was modelled (Fig. 6). Using reasonably constant magnetic susceptibilities ranging from  $90\text{--}110 \times 10^{-5}$  cgs units, a good fit between the observed data and theoretical profile was achieved. The resultant model simulates a basement ridge at depths of 520-550m below ground level. Towards the east, the basement deepens gradually to a depth of ~2200m. To the west, depth to basement increases dramatically from ~1500 to 3700m indicating a down faulted block. The fault is located just offshore.

### **Aeromagnetic Line 176/171**

The data define a simple curve (Fig. 7) suggestive of a relatively homogeneous basement, shallower to the west and deeper to the east separated by a magnetically quiet zone, possibly a basin. A continuation of the broad aeromagnetic high inland from Cape Cassini is also traversed by Line 176/171.

This western portion of the survey line was modelled to determine whether the basement here was of similar depths to those calculated for Line 210.

Susceptibilities similar to those used in the modelling of Line 210 were chosen and ranged from  $80\text{--}125 \times 10^{-5}$  cgs units. As in Line 210, the model suggested a basement ridge coincident with the magnetic high and shallowing gently to the east but more sharply to the west. The shallowest basement occurs at ~750m below ground level, slightly deeper but still of the same order as depths produced for Line 210. Thus, the north-south trending aeromagnetic high coincides with an interpreted basement ridge of broadly constant depth averaging ~630m, but with a minimum of ~520m on Line 210.

### **Aeromagnetic Line 9170**

This north-south tie-line was also chosen for its proximity to the Hummocky Point-Cape Cassini area, but unfortunately due to the large spacing between tie-lines, this traverse is east of the magnetic maximum.

The susceptibilities used in this model range from  $75\text{--}160 \times 10^{-5}$  cgs units producing a moderate fit with the observed data (Fig. 8). The model fit has two main features, a relatively deep (~1000m) homogeneous Proterozoic body to the south and a shallower body to the north which is much more variable both in depth (ranging from ~830-340m below ground/sea level) and susceptibility ( $35\text{--}160 \times 10^{-5}$  cgs units). The two regions are separated by a fault which is approximately coincident with the coastline. Although this model gives quite large depths to the basement onshore (c.1000m), it must be remembered



that this line is positioned over 2km away from and oriented parallel to the aeromagnetic maximum.

#### **Aeromagnetic Line 9141**

This is a north-south orientated tie-line selected to model the Cape D'Estaing area, however, once again the tie line is 2km west of the magnetic maximum. The flight line also cuts an interesting magnetic low which was modelled in two ways:- as a granite intrusion, and as a rift in the basement.

Figure 9 portrays the intrusive model for line 9141. For this model, the depths to basement were kept constant at ~350 to 550m below ground level, and rocks with low magnetic susceptibilities of  $70 \times 10^{-5}$  cgs units in the area of the low suggest a relatively non-magnetic basement body such as a granite or a gneiss. Other susceptibilities ranged from 85-140  $\times 10^{-5}$  cgs units, indicative of granites and granulites. A particularly high susceptibility of  $180 \times 10^{-5}$  cgs units for a thin body was interpreted as a basic granulite.

The alternative rift model is displayed in Figure 10. Uniform susceptibilities of  $130 \times 10^{-5}$  cgs units were maintained under the magnetic low and depth was altered until a good model-curve fit was achieved. Several faulted blocks combine to produce an overall displacement of almost 1500m, the bottom of the rift reaching a depth of ~2150m below ground level. The width of the rift zone is hard to determine accurately, but a figure between 8 and 10km is suggested.

Although the rift model is both the preferred

geological explanation and the better fitting model, the intrusive model has been retained for two reasons.

Firstly, it is a viable alternative model and secondly, it displays the wide variety of possible models which still give a good mathematical fit despite their configurational differences. This illustrates the necessity for good geological constraints when geophysical modelling.

#### **Aeromagnetic Line 9120**

This north-south orientated line intersects the east-west Line 240 in the Bald Rock area. At the point where the lines intersect, a similar susceptibility of  $117 \times 10^{-5}$  cgs units was chosen. The southern end of the line is adjacent to Line 9122 so similar depths and susceptibilities were used, providing further constraints.

The model (Fig. 11) produced a minimum basement depth of only ~140m below ground level for the Bald Rock aeromagnetic high; this is comparable with 210m calculated from Line 240. Southwards, the basement deepens through down-faulting to about 1800m at the limit of the model. Offshore to the north, the basement is magnetically inhomogeneous and relatively shallow, with modelled depths ranging from ~330 to 540m below sea level.

## **Aeromagnetic Line 9122**

This north-south oriented line slightly overlaps Line 9120 and was chosen to model both the large aeromagnetic high southwest of Kingscote and the Cygnet Fault. The observed magnetic profile displays a large magnetic high and several small superimposed features on its southern flank (Fig. 12). The curve was interpreted initially as a representing deep basement block, producing the dominant feature, with several shallower, steeply dipping units within the overlying cover sequence producing the small anomalies.

Using the curve-fitting and data-manipulation abilities of the Toolkit application, a polynomial was calculated to fit the major curve. Its gentle slopes imply relatively deep basement. Basement effects were then subtracted from the data set, leaving a residual curve which was assumed to be derived from shallower bodies.

The final model is interpreted as deep basement to the south covered by steeply dipping Kanmantoo Group metasediments. A major fault zone separates the Kanmantoo Group from the Kangaroo Island Group to the north. This is interpreted as a syn-depositional listric fault at the time of sedimentation, but changing to a high angle reverse fault during orogenesis. The contemporary expression of this fault zone is the Cygnet Fault, a 2-7 km wide zone that includes a visible fault scarp, foliated to mylonitic, fine-grained quartzites and schists, and associated Pb, Zn Ag and Au mineralization (McCallum, 1991).

To the north is a zone, also modelled in the adjoining Line 9120, which has poor geological constraints. Unfortunately this could not be further explored due to limitations in the maximum number of bodies available in the Toolkit program. Either the zone may represent a failed rift basin (as interpreted) or the basement may have lower magnetic susceptibility.

## **Gravity Line 3A**

A gravity survey, close to magnetic Line 9122, was modelled to gain additional information on the basement configuration and the nature of the Cygnet Fault. The interpreted model is displayed in both Figures 13 and 14, but note the different scales used to highlight the basement configuration (Fig. 13) and near-surface features (Fig. 14).

Exposures and subsurface drilling data indicate presence of Tertiary sediments, Jurassic volcanics and Permian sediments. These have been included in the model, as shown in detail in Fig. 14. A basin north of the Cygnet Fault has a sedimentary fill of ~300m.

For the modelling of the gravity profile, the limit to the number of bodies available within the program handicapped the realism accomplished and hence only an approximate match between the observed data and theoretical profile was obtained. However, very good agreement exists between the theoretical gravity and magnetic models, supporting the validity of the geological interpretation. In particular, the Cygnet Fault Zone forms the major boundary between relatively shallow basement to the north and a tightly

folded cover sequence overlying very deep basement to the south.

### **Gravity Line 2A**

This line, between American River and Penneshaw, is along a topographically low-lying portion of the island. Both to the west and east are prominent exposures of Kanmantoo Group metasediments, but the intervening area around Pennington Bay and Pelican Lagoon contains only Quaternary sedimentary exposures (Fig. 2).

The gravity data display a prominent gravity low, and the modelling suggests the presence of a small but significant sedimentary basin overlying the Kanmantoo Group (Fig. 15). Quaternary, Tertiary and Permian strata have a probable combined total thickness of 650m. The basin's geometry is indicative of an elongate Permian glacial valley.

### **SUMMARY**

Prominent aeromagnetic highs occur over northern Kangaroo Island inland from Cape Cassini and southwest of Kingscote. Both areas represent a continuation, but at greater depth, of shallow crystalline basement of the Palaeoproterozoic Lincoln Complex within Investigator Strait and on southern Yorke Peninsula. The basement is a southern extension of the Gawler Craton.

Inland from Cape Cassini, a magnetic high is consistent with a north-south ridge of basement with a crest at ~520m below ground level (Fig. 16). Depth

to basement increases quickly both to the west and east of the ridge. Cape D'Estaing and Bald Rock near Emu Bay both coincide with the margins of aeromagnetic highs that are principally located offshore. Basement is shallowest at Bald Rock and is only ~150-220m below ground level. Depths to basement increase quickly southwards away from the coast in both areas.

Southwest of Kingscote, the broad aeromagnetic high reflects a block of crystalline basement at ~2000m below ground level. The northern flank of the high has small, superimposed anomalies due to outcropping Jurassic tholeiitic basalts.

The southern extension of relatively shallow crystalline basement is terminated by a complex tectonic zone up to 7.5 km wide and consisting of both ductile shears and brittle faults. Crystalline basement is downfaulted to the south across a series of shears to a depth approaching 10 km. Listric faulting synchronous with sedimentation controlled the distribution and thickness of Cambrian strata, in a situation analogous to the Torrens Hinge Zone and its influence on Adelaidean strata of the Stuart Shelf and Adelaide Geosyncline. In addition to controlling the nature and thickness of Cambrian sedimentation, this zone also acted as a major subdomain boundary during the subsequent Delamerian Orogeny, along which reverse faulting and thrusting occurred under the compressive stress regime.

The sedimentary cover over the crystalline basement to the north of the Cygnet and Snelling Faults is part of the Cambrian Kangaroo Island Group of the

Stansbury Basin. Well exposed in coastal sections, the sequence has been gently folded and metamorphosed to low greenschist facies.

At both Cape D'Estaing and Bald Rock, very coarse clastics of the White Point Conglomerate are exposed and suggest the Cambrian sequence is incomplete due to shallow basement. However, over the basement ridge inland from Cape Cassini, exposed units are the Stokes Bay Sandstone and Mt McDonnell Formation which are stratigraphically the two lowermost units in the sequence. Depth to basement of ~520-750m infers a considerable thickness of Mt McDonnell Formation and/or older, unknown Cambrian strata. Sedimentary dips in the area, especially near Hummocky Point, are subhorizontal and make the area ideal as a drilling target to appraise both the nature of the Cambrian cover and crystalline basement.

The thickness of Cambrian cover in other areas north of the Cygnet Fault is generally between 1000 and 2000m.

South of the Cygnet Fault, the cover sequence comprises typical Kanmantoo Group metasandstones and phyllites. Sediments are tightly folded, multiply deformed and metamorphosed to upper greenschist-low amphibolite facies during the Delamerian Orogeny.

Subsequent reactivation of the Cygnet-Snellings fault zone along the southern margin of the craton resulted in ductile shearing and thrusting. More recent reactivation has produced the brittle Cygnet Fault.

Preserved to the north is a shallow basin containing Permian, Jurassic, Tertiary and Quaternary strata.

## REFERENCES

- Daily, B., Milnes, A.R., Twidale, C.R. and Bourne, J.A., 1979. Geology and Geomorphology. *In*: Tyler, M.J., Twidale, C.R. and Ling, J.K. (Eds). *Natural History of Kangaroo Island*. Royal Society of South Australia. pp. 1-38.
- Finlayson, D.M., 1973. Isomagnetic maps of the Australian region for the Epoch 1970.0. *Bureau of Mineral Resources, Geology and Geophysics, Australia, Report 159*.
- Flint R.B. and Parker, A.J., 1982. Tectonic map of South Australia. *South Australia. Geological Survey. Maps of South Australia Series*, 1:2 000 000.
- McCallum, W.S., 1991. Geological Investigations and drilling, Parndana area, Kangaroo Island, 1989-1990. South Australia Dept. of Mines and Energy. Report Book 91/23.
- Mortimer, G.E., Cooper, J.A. and Oliver, R.L., 1979. Petrological and petrochemical evolution of the 1.823 B.Y. Donington Granitoid Suite of the southeast Eyre Peninsula. *In*: Parker, A.J. (Compiler). *Symposium on the Gawler Craton, Extended Abstracts*. Geological Society of Australia, pp. 37-38.

- Mortimer, G.E., Cooper, J.A. and Oliver, R.L., 1986.  
The geochronological and geochemical evolution  
of the Proterozoic Lincoln Complex, Eyre  
Peninsula. *Geological Society of Australia.  
Abstracts*, 15: 140-141.
- Mortimer, G.E., Cooper, J.A. and Oliver, R.L., 1988.  
Proterozoic mafic dykes near Port Lincoln, South  
Australia: Composition, age and origin.  
*Australian Journal of Earth Sciences*, 35: 93-110.
- Rankin, L.R., Flint, R.B. and Belperio, A.P., 1991.  
Precambrian geology of islands in the Investigator  
Strait area, South Australia. *South Australia.  
Department of Mines and Energy. Report Book*,  
91/57.
- Webb, A.W., Thomson, B.P., Blissett, A.H., Daily,  
S.J., Flint, R.B. and Parker, A.J., 1986.  
Geochronology of the Gawler Craton, South  
Australia. *Australian Journal of Earth Sciences*,  
33: 119-143.

## APPENDIX A

**Magnetic Susceptibilities For Various Rock Specimens**

R.S.#	Comments	Susceptibility SI	Units cgs (*10 <sup>-5</sup> )
QUATERNARY (ascending RS number)			
6325 RS 15	Calcarenite	0.00012	1.0
6326 RS 880	Limestone	0.00000	0.0
6326 RS 1115	Limestone	0.00002	0.2
6426 RS 33	Bridgewater Formation	0.00002	0.2
6426 RS 47	Bridgewater Formation	0.00001	0.1
6426 RS 48	Bridgewater Formation	0.00200	15.9
6426 RS 49	Bridgewater Formation	0.00210	16.7
6426 RS 50	Bridgewater Formation	0.00001	0.1
6426 RS 85	Hindmarsh Clay?	0.00023	1.8
6426 RS 187	Glanville Formation	0.00009	0.7
6426 RS 198	Limestone	0.00001	0.1
6426 RS 199	Bridgewater Formation	0.00002	0.2
6426 RS 203	Glanville Formation?	0.00087	6.9
6426 RS 217	Glanville Formation	0.00005	0.4
6426 RS 217	Glanville Formation - sand	0.00016	1.3
TERTIARY			
6326 RS 881	Pliocene - limestone	0.00001	0.0
6326 RS 882b	Silcrete	0.00016	1.3
6326 RS 1119	Late Tertiary - limestone	0.00000	0.0
6326 RS 1120	Tertiary?	0.00015	1.2
6426 RS 66	Pliocene? - limestone	0.00000	0.0
6426 RS 89	Pliocene	0.00027	2.1
6426 RS 91	Eocene - limestone	0.00002	0.2
6426 RS 200	Pliocene - limestone	0.00001	0.1
6426 RS 207	Eocene? - limestone	0.00000	0.0
6426 RS 209	Pliocene? - limestone	0.00000	0.0
JURASSIC			
6426 RS 94	Basalt	0.00490	39.0
6426 RS 224	Claystone	0.00001	0.0
6426 RS 225	Sand	0.00004	0.3
6426 RS 226	Sandstone chip	0.00015	1.2
6426 RS 226	Loose sand	0.00027	2.1
6526 RS 89	Basalt	0.00330	26.3

# PERMIAN

6426 RS 69	Diamictite	0.00002	0.2
6426 RS 88	Diamictite	0.00001	0.1
6426 RS 93	Diamictite	0.00013	1.0
6426 RS 212	Boulder A within diamictite	0.00130	10.3
6426 RS 212	Boulder B within diamictite	0.00240	19.1
6426 RS 213	Boulder within diamictite	0.00185	14.7

# ORDOVICIAN

6426 RS 59	Dolerite	0.00170	13.5
6426 RS 60	Dolerite	0.00082	6.5
6526 RS 50	Granite	0.00007	0.6
6526 RS 52	Granite	0.00012	1.0
6526 RS 70	Pegmatite	0.00003	0.2
6526 RS 87	Pegmatite	0.00002	0.2
6526 RS 88	Pegmatite	0.00004	0.3

# CAMBRIAN - KANGAROO ISLAND GROUP (descending stratigraphic sequence)

6426 RS 228	Boxing Bay Formation	0.00068	5.4
6426 RS 229	Boxing Bay Formation - limestone	0.00007	0.6
6426 RS 230	Boxing Bay Formation - limestone	0.00003	0.2
6426 RS 238	Boxing Bay Formation	0.00012	1.0
6326 RS 884	White Point Conglomerate	0.00001	0.1
6426 RS 233	White Point Conglomerate	0.00006	0.5
6426 RS 233	White Point Conglomerate	0.00010	0.8
6426 RS 234	White Point Conglomerate	0.00003	0.2
6426 RS 235	White Point Conglomerate	0.00014	1.1
6326 RS 1118	Stokes Bay Sandstone	0.00018	1.4
6326 RS 1121	Stokes Bay Sandstone	0.00011	0.9
6326 RS 1125	Stokes Bay Sandstone	0.00017	1.4
6326 RS 889	Mt McDonnell Formation - limestone	0.00005	0.4
6326 RS 889	Mt McDonnell Formation - limestone	0.00010	0.8
6326 RS 889	Mt McDonnell Formation - shale	0.00010	0.8
6326 RS 892	Mt McDonnell Formation	0.00011	0.9
6326 RS 893	Mt McDonnell Formation	0.00016	1.3
6326 RS 1123	Mt McDonnell Formation - limestone	0.00008	0.6
6326 RS 1124	Mt McDonnell Formation - limestone	0.00006	0.5

# CAMBRIAN - KANMANTOO GROUP (descending stratigraphic sequence)

6325 RS 12	Sandstone	0.00059	4.7
6325 RS 13	Sandstone	0.00088	7.0
6326 RS 1116	Quartzite	0.00001	0.1
6326 RS 1117	Mylonite	0.00002	0.2
6426 RS 206		0.00016	1.3
6325 RS 10	Middleton Sandstone (h.min-rich sst)	0.02800	222.8

6425 RS	2	Middleton Sandstone (h.min-rich sst)	0.03100	246.7
6425 RS	3	Middleton Sandstone	0.00003	0.2
6425 RS	9	Middleton Sandstone	0.00003	0.2
6526 RS	57	Middleton Sandstone	0.00017	1.4
6526 RS	60	Middleton Sandstone?	0.00880	70.0
6526 RS	103	Middleton Sandstone	0.00042	3.3
6426 RS	31	Petrel Cove Formation	0.00016	1.3
6426 RS	32	Petrel Cove Formation	0.00014	1.1
6426 RS	40	Petrel Cove Formation	0.00011	0.9
6426 RS	41	Petrel Cove Formation	0.00016	1.3
6526 RS	99	Petrel Cove Formation	0.00018	1.4
6526 RS	96	Balguhiddar Formation?	0.00019	1.5
6426 RS	83	Tunkalilla Formation?	0.00016	1.3
6426 RS	62	Tapanappa Formation - sandstone	0.00012	1.0
6526 RS	71	Tapanappa Formation - phyllite	0.00005	0.4
6426 RS	72	Tapanappa Formation	0.00180	14.3
6426 RS	73	Tapanappa Formation	0.00009	0.7
6426 RS	74	Tapanappa Formation - conglomerate	0.00006	0.5
6426 RS	90	Tapanappa Formation	0.00013	1.0
6426 RS	188	Tapanappa Formation	0.00008	0.6
6526 RS	68	Tapanappa Formation	0.00014	1.1
6526 RS	86	Tapanappa Formation	0.00011	0.9
6526 RS	95	Tapanappa Formation	0.00330	26.3
6526 RS	73	Talisker Calcsiltstone	0.00011	0.9
6526 RS	85	Backstairs Passage Formation	0.00010	0.8
6526 RS	83	Carrackalinga Head Formation	0.00016	1.3
6526 RS	84	Carrackalinga Head Formation	0.00005	0.4

PROTEROZOIC - LINCOLN COMPLEX  
(ascending RS numbers)

6127 RS	1	Felsic gneiss, South Neptune Island	0.00790	62.9
6127 RS	2	Granulite, South Neptune Island	0.00350	27.9
6127 RS	3	Granulite, North Neptune Island	0.01050	83.6
6127 RS	6	Gneiss, North Neptune Island	0.00310	24.7
6127 RS	9	Felsic Granulite, North Neptune Island	0.01050	83.6
6127 RS	10	Granulite, North Neptune Island	0.04200	334.2
6127 RS	12	Gneiss, North Neptune Island	0.00280	22.3
6127 RS	13	Granite, North Neptune Island	0.00395	31.4
6127 RS	14	Felsic granulite, North Neptune Island	0.00360	28.6
6127 RS	17	Gneiss, north of North Neptune Island	0.01450	115.4
6127 RS	18	Granulite, north of North Neptune Island	0.00069	5.5
6127 RS	31	Felsic gneiss, South Neptune Island	0.00160	12.7
6127 RS	32	Gneiss, South Neptune Island	0.00250	19.9
6127 RS	33	Basic granulite, South Neptune Island	0.00029	2.3
6127 RS	34	Basic granulite, South Neptune Island	0.03800	302.4
6127 RS	35	Basic granulite, South Neptune Island	0.03300	262.6
6127 RS	42	Granite, South Neptune Island	0.01050	83.6
6127 RS	43	Mafic granulite, South Neptune Island	0.00057	4.5
6127 RS	44	Granodiorite, South Neptune Island	0.01500	119.4
6127 RS	45	Charnockite, South Neptune Island	0.01100	87.5



6127 RS	46	Granodiorite, Wedge Island	0.02550	202.9
6127 RS	47	Dolerite, Althorpe Island	0.00670	53.3
6127 RS	48	Granite, Wedge Island	0.01400	111.4
6127 RS	49	Metadolerite, Wedge Island	0.00440	35.0
6127 RS	50	Granite, Wedge Island	0.00865	68.8
6226 RS	131a	Diorite, Investigator Strait, Fix 121	0.01850	147.2
6226 RS	131b	Diorite, Investigator Strait, Fix 121	0.00615	48.9
6227 RS	1	Dolerite, Althorpe Island	0.00970	77.2
6227 RS	2	Gneiss, Althorpe Island	0.01200	95.5
6227 RS	3	Granulite, Althorpe Island	0.01150	91.5
6227 RS	4	Gneiss, Althorpe Island	0.00056	4.5
6227 RS	5	Granulite, Althorpe Island	0.00460	36.6
6227 RS	7	Gneiss, Seal Island	0.01100	87.5
6227 RS	8	Metadolerite, Seal Island	0.01150	91.5
6227 RS	9	Metadolerite, Seal Island	0.00077	6.1
6227 RS	15	Gneiss, Gleesons Landing	0.00380	30.2
6227 RS	16	Gneiss, Daly Head	0.00300	23.9
6227 RS	17	Gneiss, Daly Head	0.00022	1.8
6227 RS	18	Gneiss, Royston Head	0.01950	155.2
6227 RS	19	Gneiss, Royston Head	0.01350	107.4
6227 RS	41	Amphibolite, Althorpe Island	0.00045	3.6
6227 RS	42	Amphibolite, Althorpe Island	0.01700	135.3
6227 RS	43	Adamellite, Althorpe Island	0.00800	63.7
6227 RS	44	Dolerite, Althorpe Island	0.00365	29.0
6227 RS	45	Mylonite, Althorpe Island	0.00038	3.0

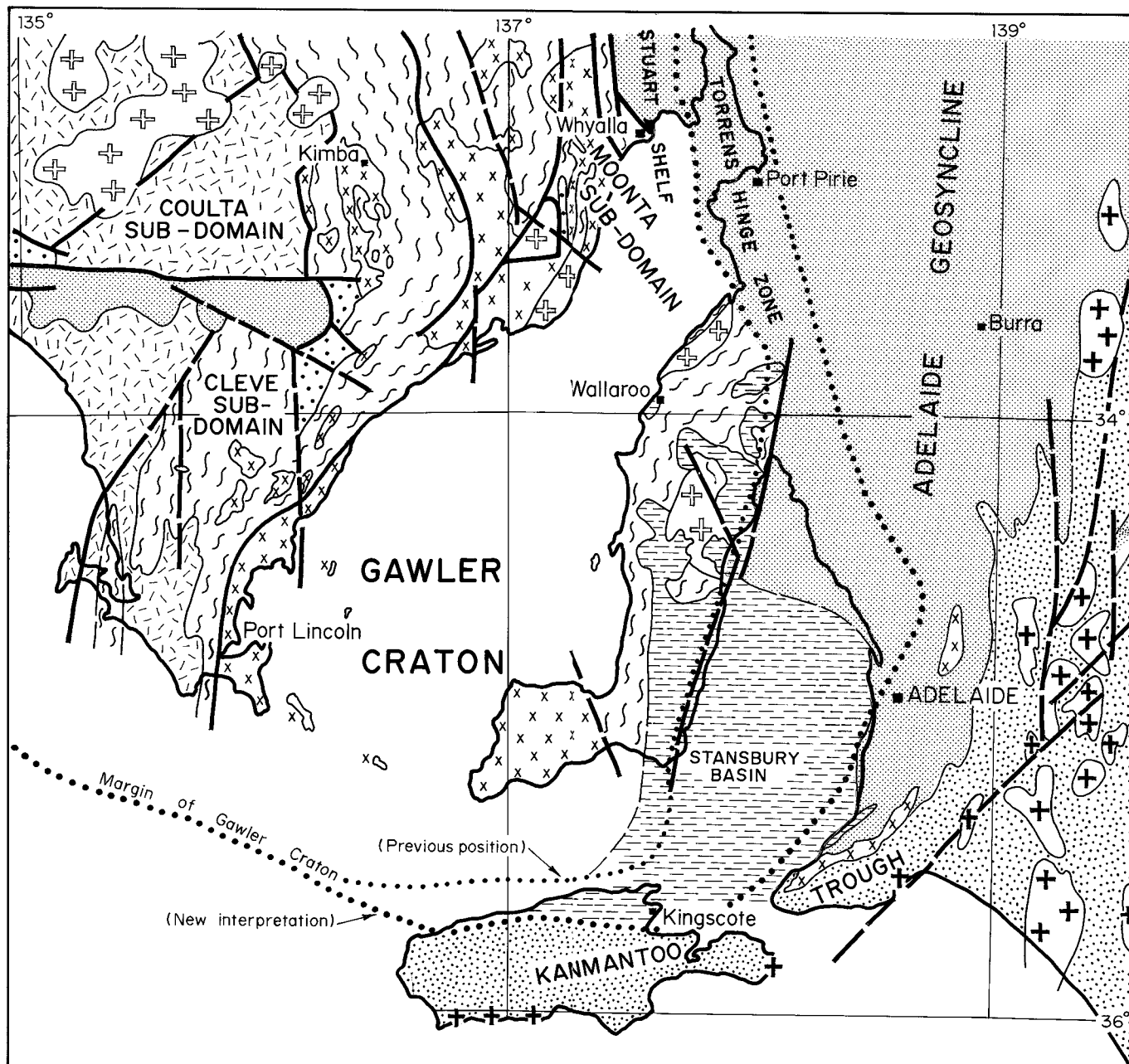
---

## APPENDIX B

### DATA DISKETTE

The enclosed 720k MS-DOS diskette contains the following 10 ASCII Files of magnetic and gravity data used in this report.

<u>Line</u>	<u>File</u>
Aeromag Line 210	AM210.PRN
Aeromag Line 9141	AM9141.PRN
Aeromag Line 240	AM240.PRN
Aeromag Line 171/176	AM171-76.PRN
Aeromag Line 9120	AM9120.PRN
Aeromag Line 9122	AM9122.PRN
Aeromag Line 9170	AM9170.PRN
Gravity Line 3A	GRAV3A.PRN
Gravity Line 2A	GRAV2A.PRN
Magnetic Susceptibility Measurements	MAGSUS.PRN



- |  |  |
|--|--|
|  | <b>KANMANTOO TROUGH</b><br>Kanmantoo Group, granite        |
|  | <b>STANSBURY BASIN</b>                                     |
|  | <b>ADELAIDE GEOSYNCLINE &amp; STUART SHELF</b>             |
|  | <b>GAWLER CRATON</b><br>Hiltaba Suite<br>Clastic sediments |
|  | Lincoln Complex  |
|  | Hutchison Group  |
|  | Sleaford Complex   |

0 50 100  
KILOMETRES

Fig. 1  
**TECTONIC PROVINCES ASSOCIATED  
WITH THE SOUTHERN  
GAWLER CRATON MARGIN**

SADME S 22438

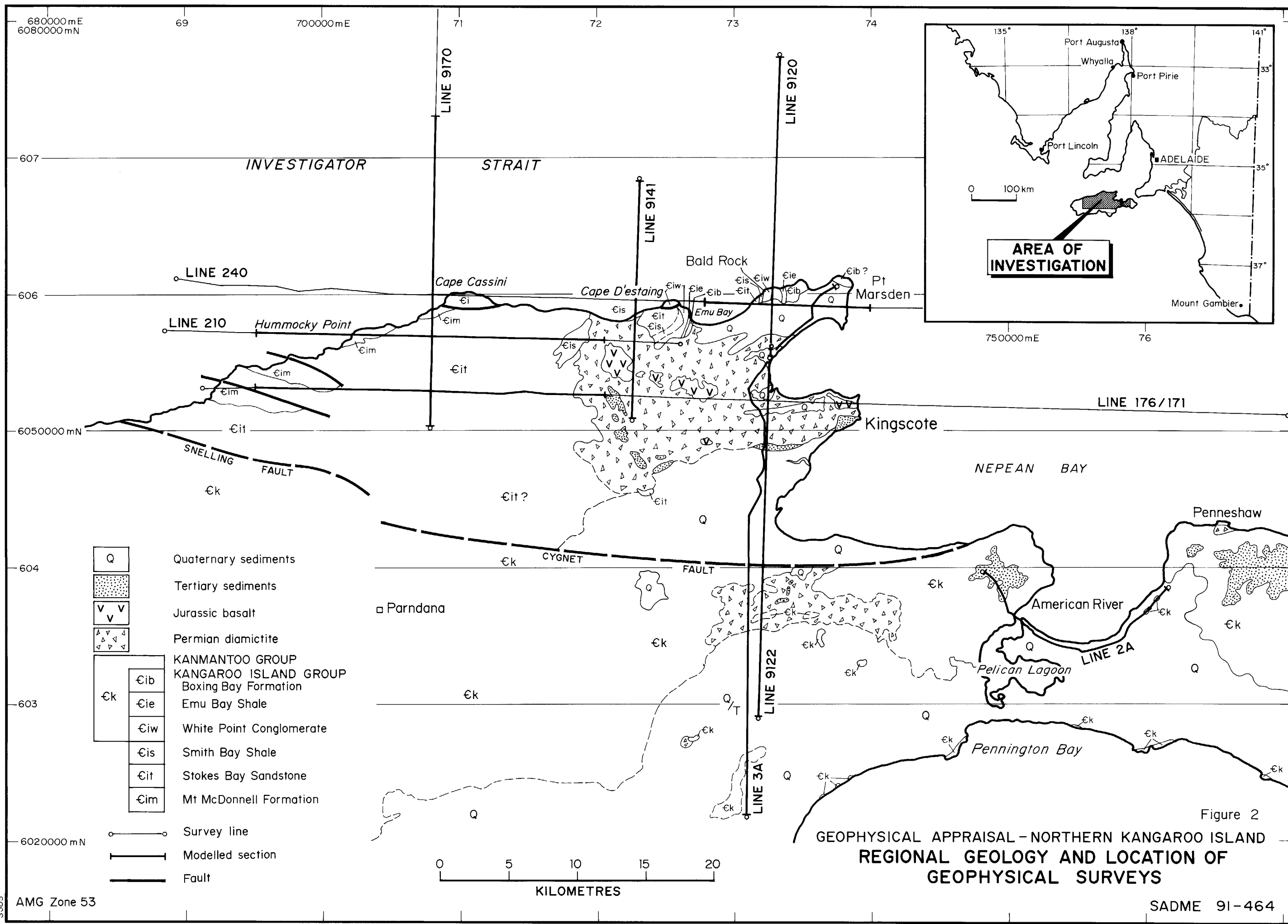
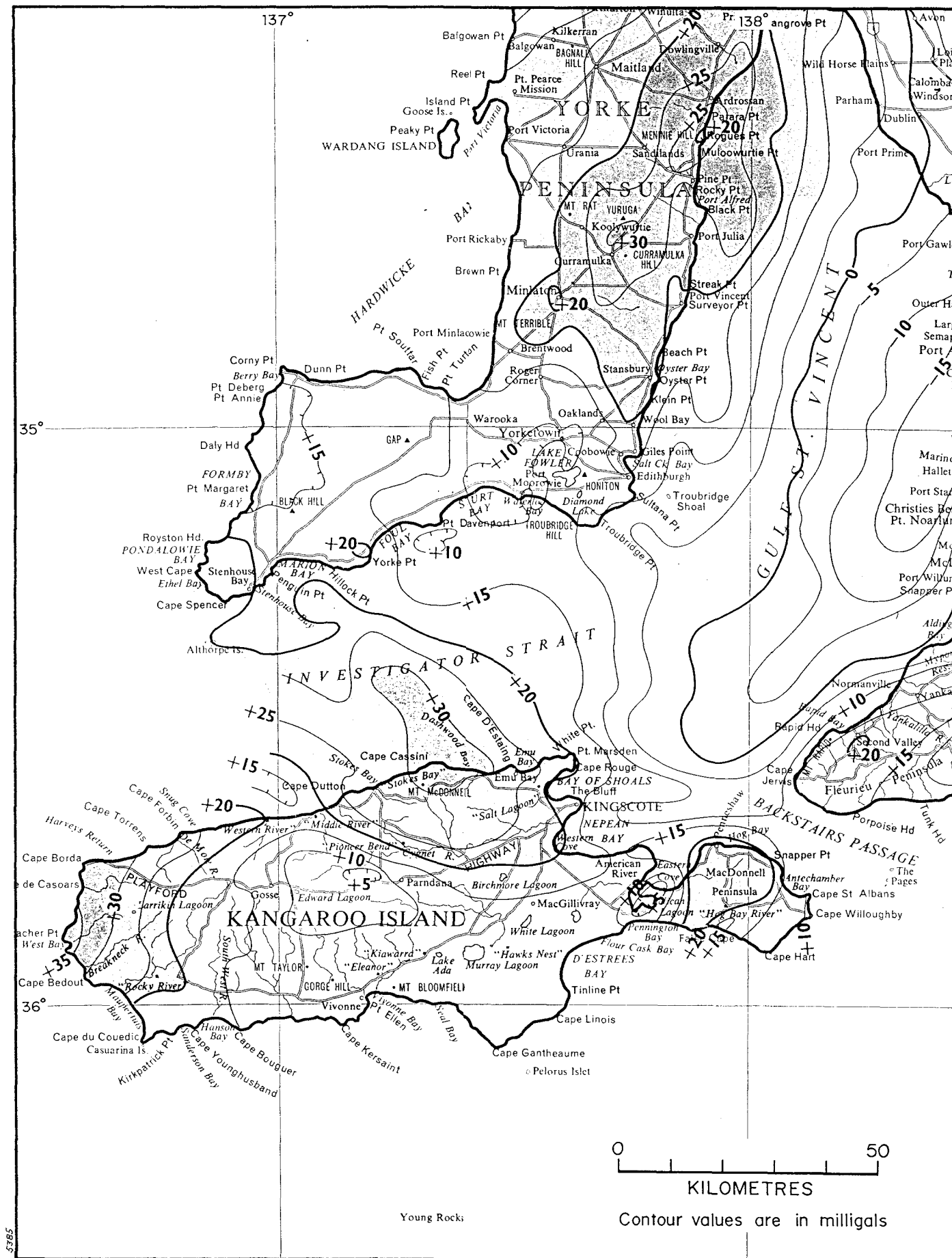


Figure 2  
 GEOPHYSICAL APPRAISAL - NORTHERN KANGAROO ISLAND  
 REGIONAL GEOLOGY AND LOCATION OF  
 GEOPHYSICAL SURVEYS

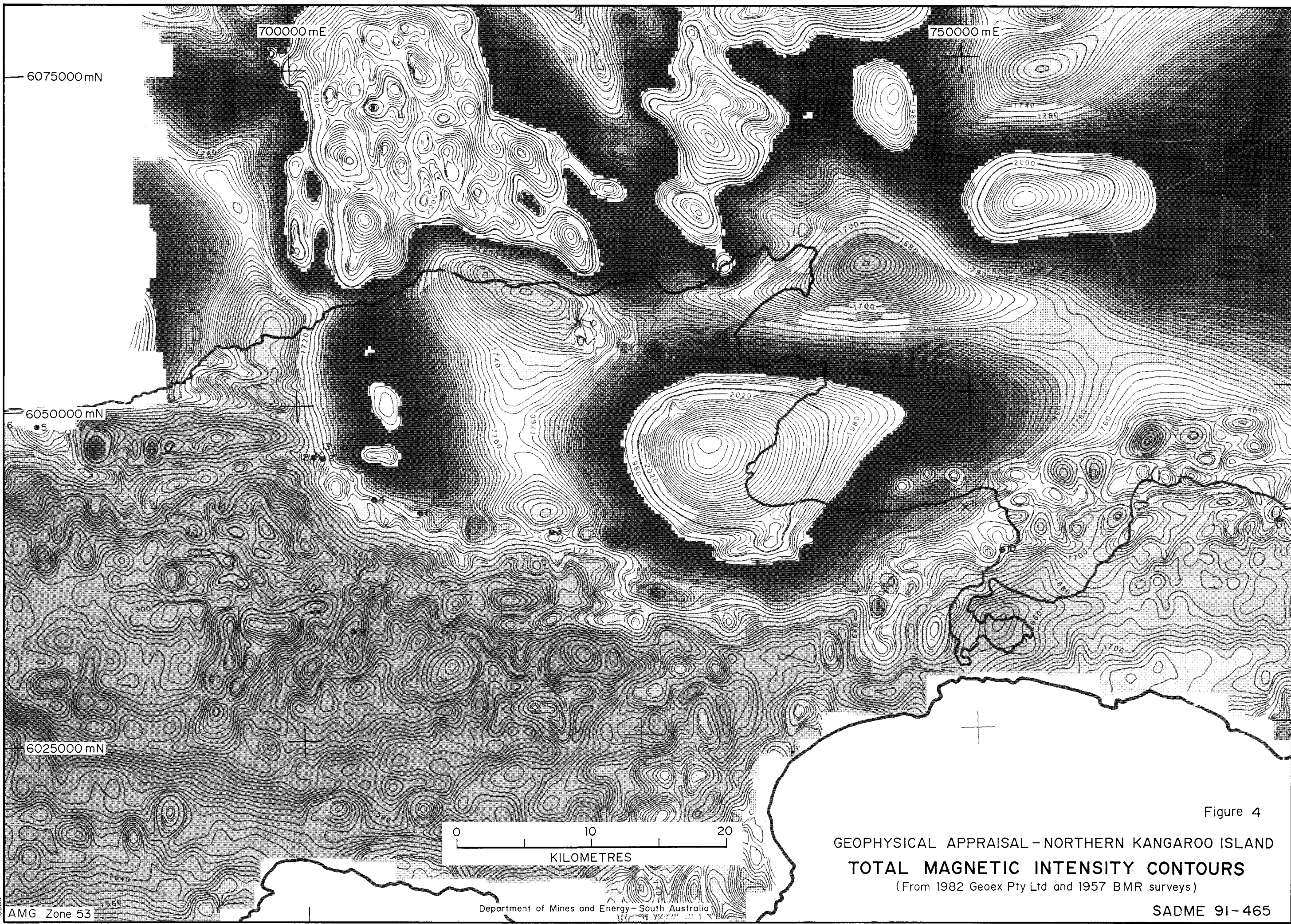


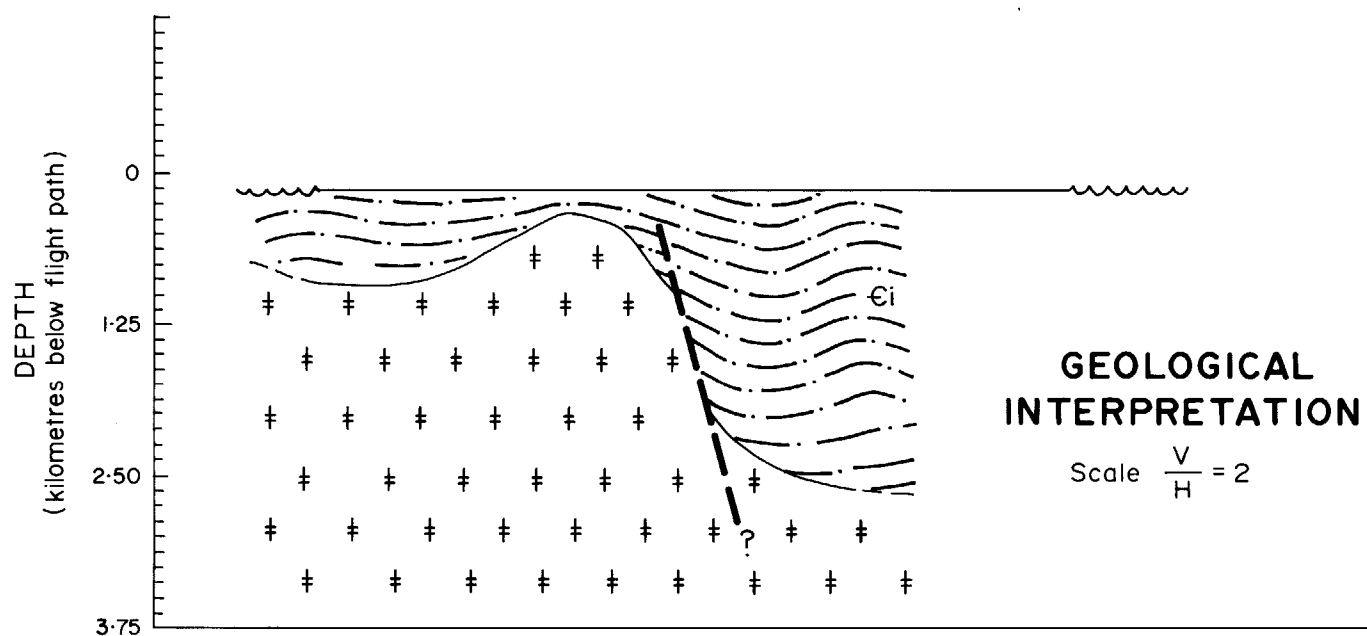
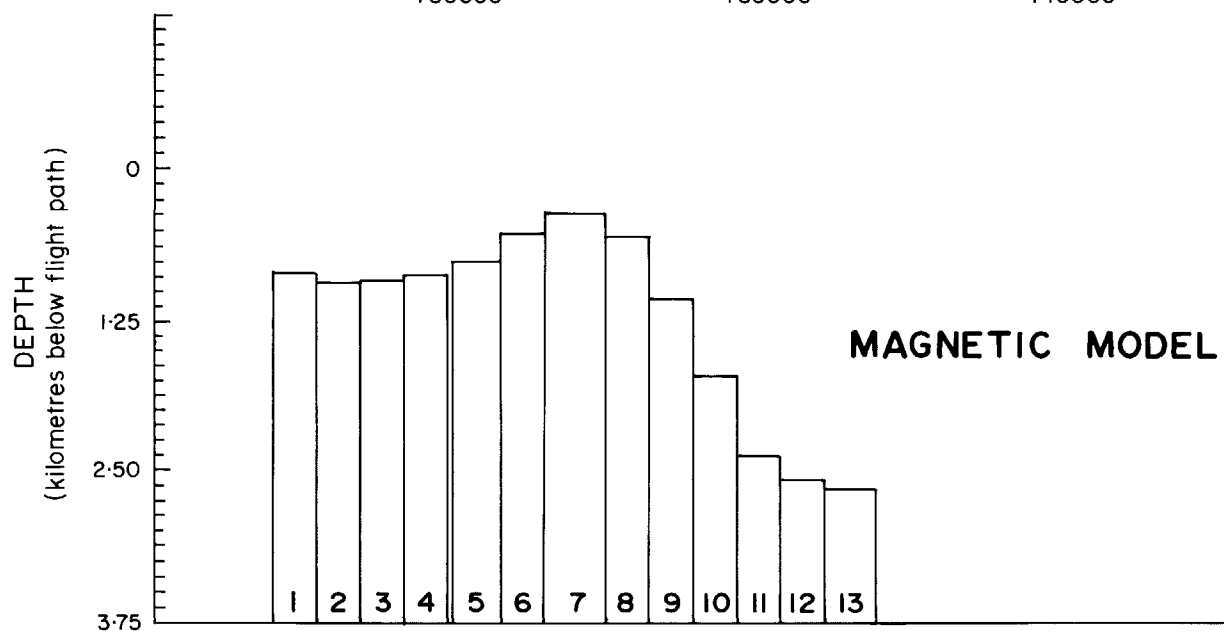
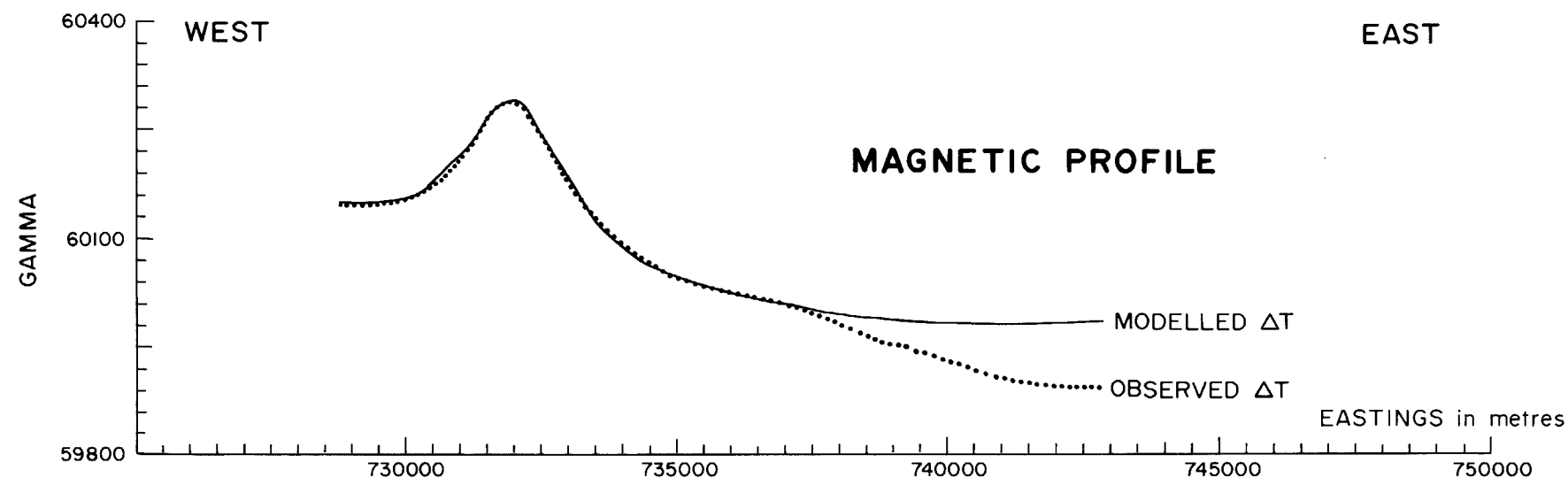
Department of Mines and Energy—South Australia

Figure 3

GEOPHYSICAL APPRAISAL - NORTHERN KANGAROO ISLAND  
BOUGUER GRAVITY CONTOURS  
SADME S22439







## MODEL SUMMARY

BODY No.	POSITION		DEPTH (m)	SUSCEPTIBILITY cgs units ( $\times 10^5$ )
	TOP LEFT	TOP RIGHT		
1	726943	727657	849	130
2	727657	728371	934	130
3	728371	729086	913	130
4	729086	729800	870	130
5	729873	730659	749	130
6	730656	731371	520	130
7	731389	732372	357	130
8	732372	733087	541	130
9	733084	733799	1066	130
10	733820	734534	1715	130
11	734522	735236	2390	130
12	735236	735950	2572	130
13	735965	736798	2650	130

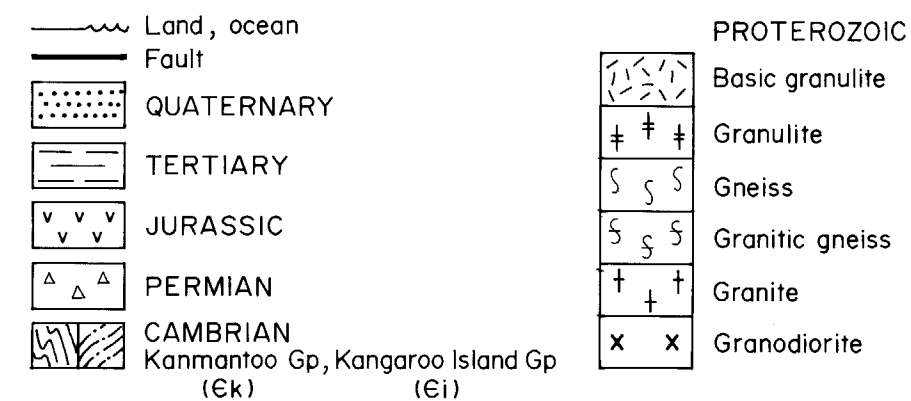
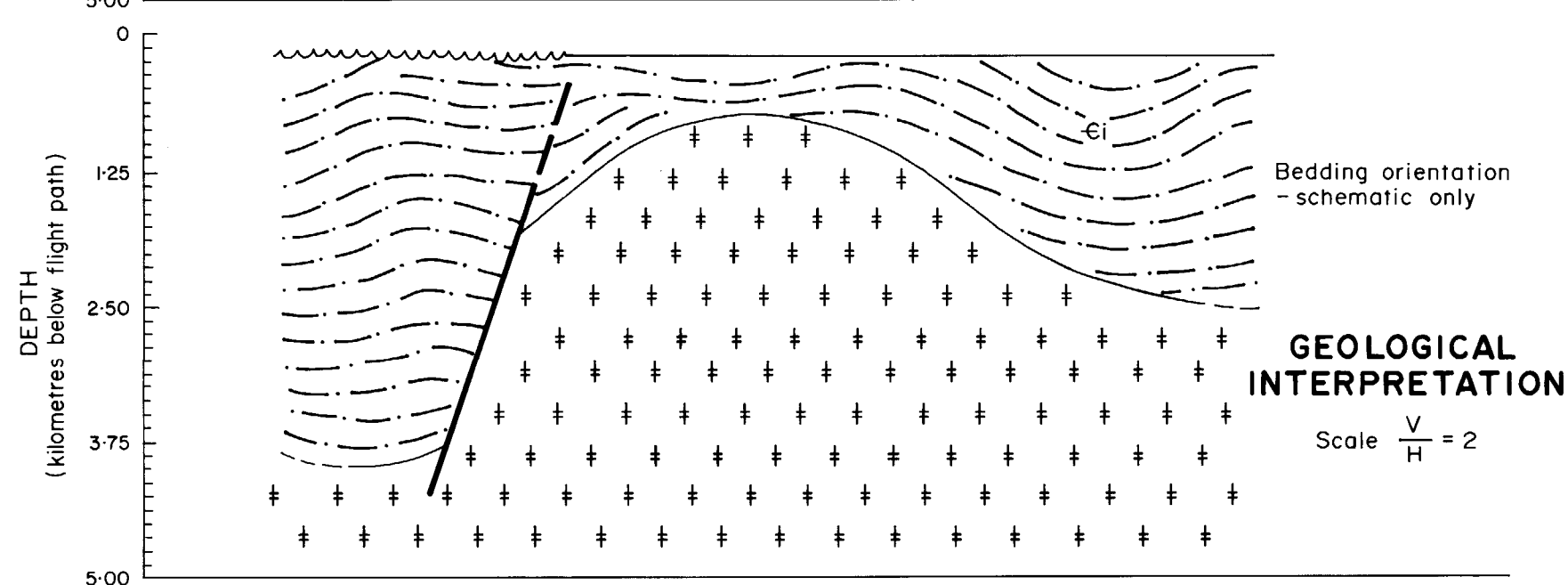
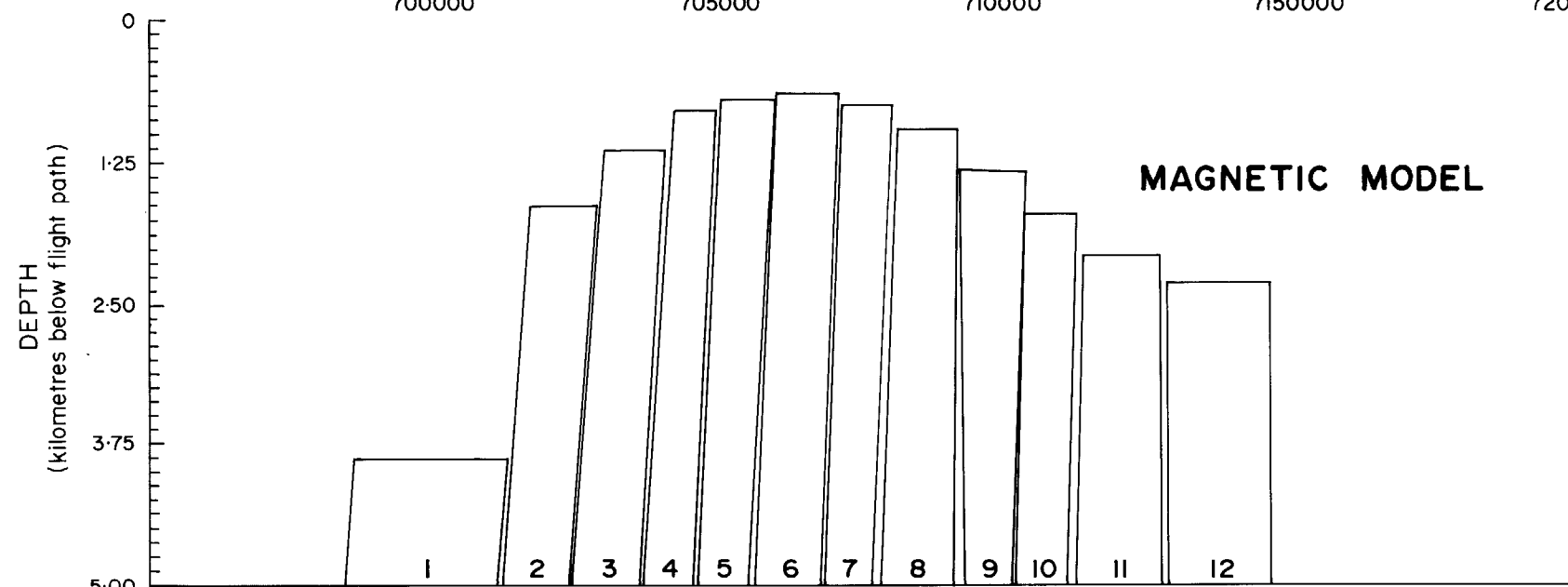
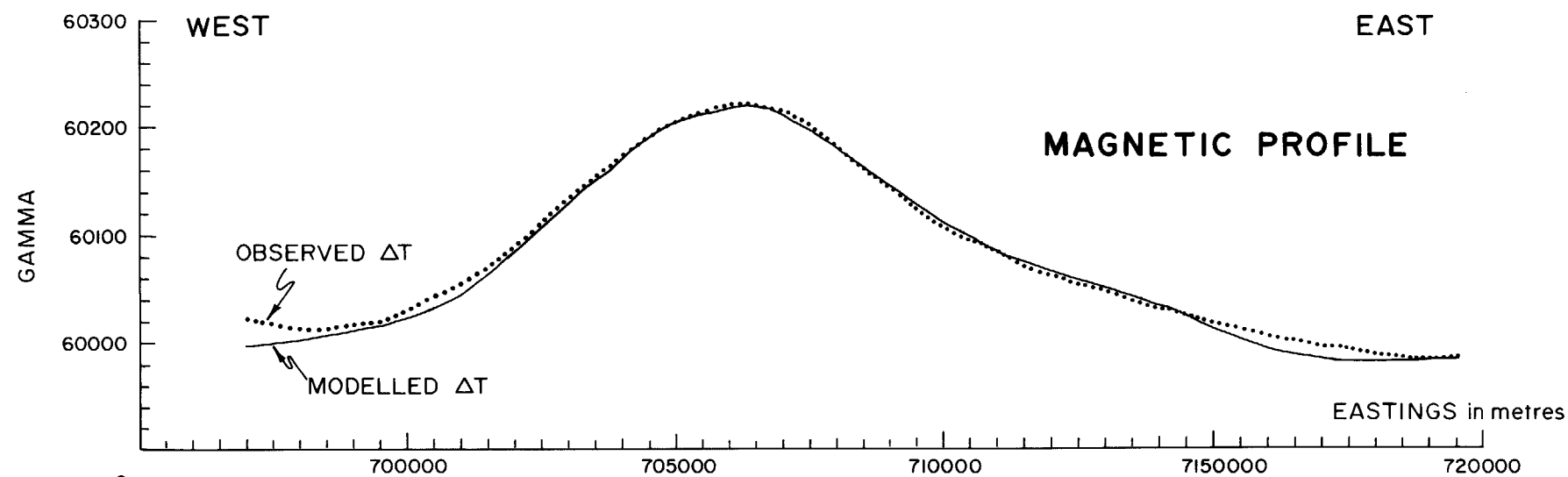


Fig. 5

**AEROMAGNETIC PROFILE  
MODEL AND GEOLOGICAL INTERPRETATION  
LINE 240**





### MODEL SUMMARY

BODY No.	POSITION		DEPTH (m)	SUSCEPTIBILITY cgs units ( $\times 10^{-5}$ )
	TOP LEFT	TOP RIGHT		
1	698589	701268	3899	80
2	701715	702876	1648	90
3	703010	704082	1161	110
4	704215	704975	813	110
5	705064	706001	717	110
6	706046	707118	669	110
7	707162	708055	766	110
8	708145	709216	989	110
9	709261	709306	1337	100
10	710422	711315	1733	100
11	711404	712744	2104	100
12	712878	714664	2351	100

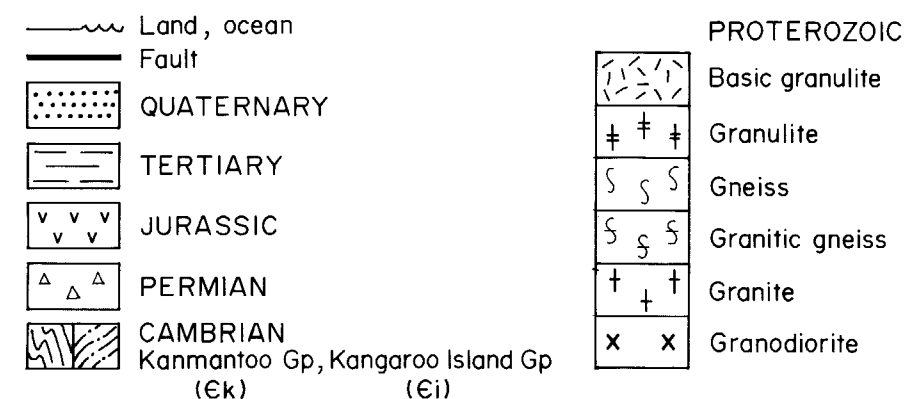
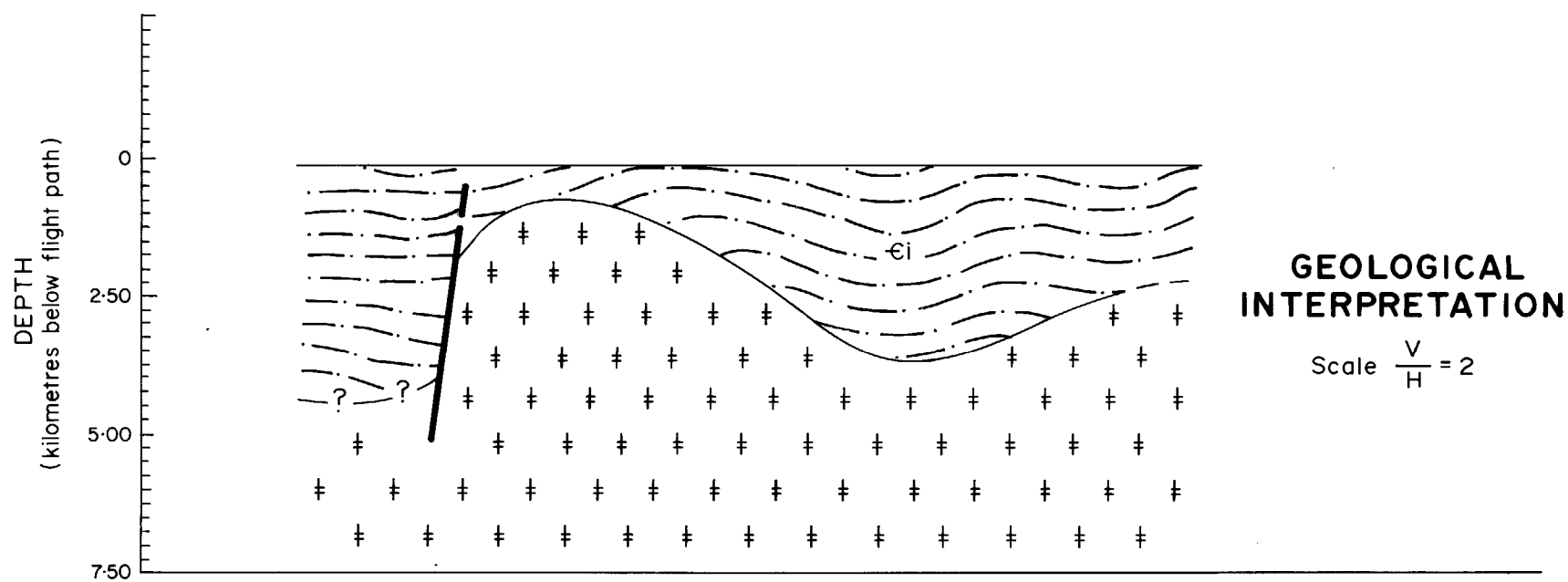
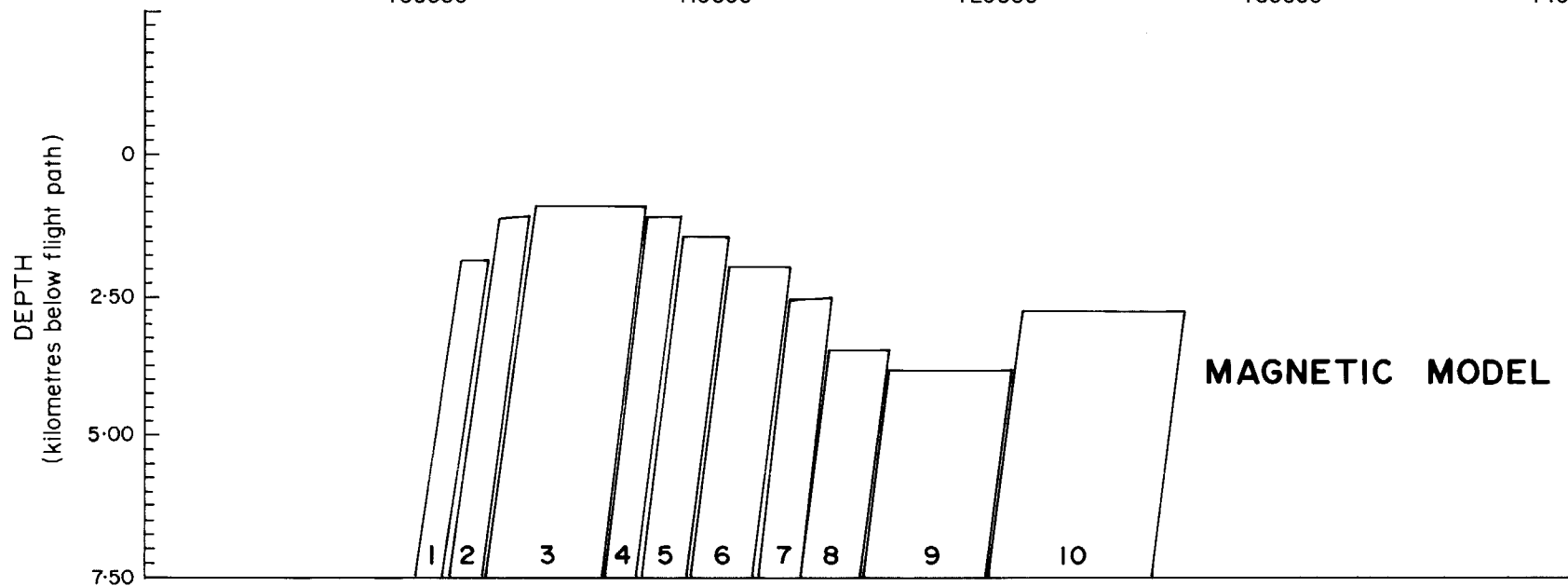
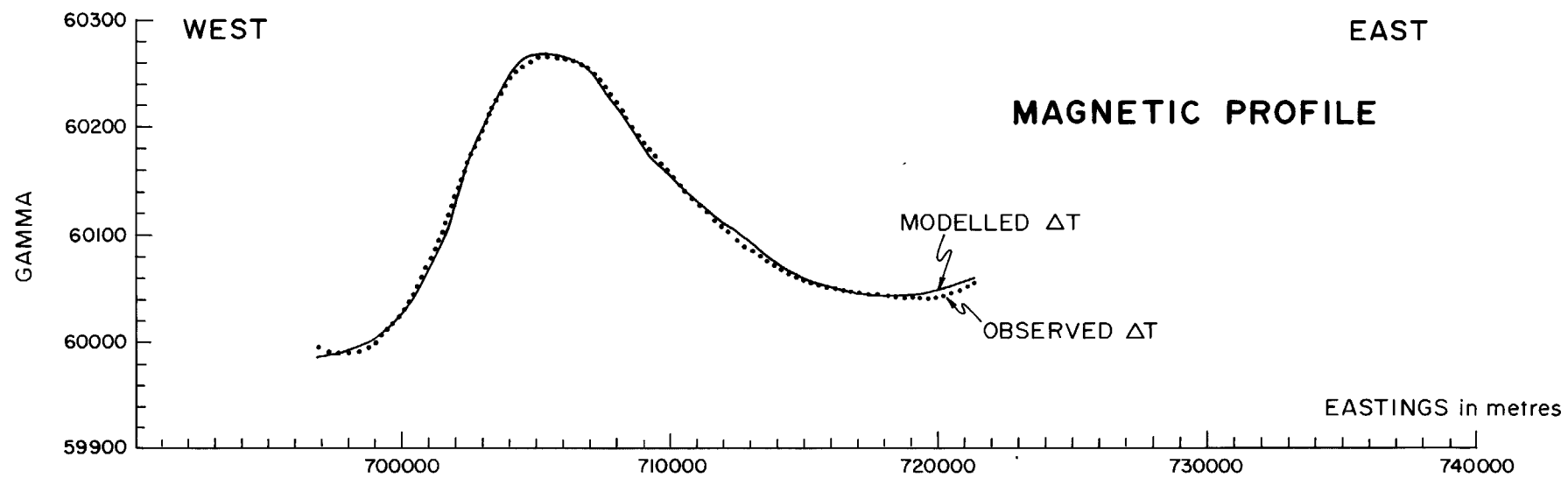


Fig. 6  
**AEROMAGNETIC PROFILE  
MODEL AND GEOLOGICAL INTERPRETATION  
LINE 210**





## MODEL SUMMARY

BODY No.	POSITION		DEPTH (m)	SUSCEPTIBILITY cgs units ( $\times 10^{-5}$ )
	TOP LEFT	TOP RIGHT		
1	701101	702030	1855	90
2	702387	703458	1092	125
3	703673	707531	892	125
4	707602	708745	1060	125
5	708817	710460	1444	110
6	710460	712603	1962	100
7	712603	714032	2513	90
8	713960	716104	3422	80
9	716104	720390	3767	80
10	720747	726463	2710	95

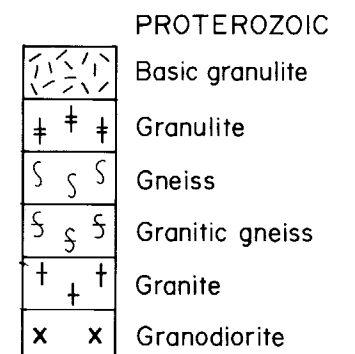
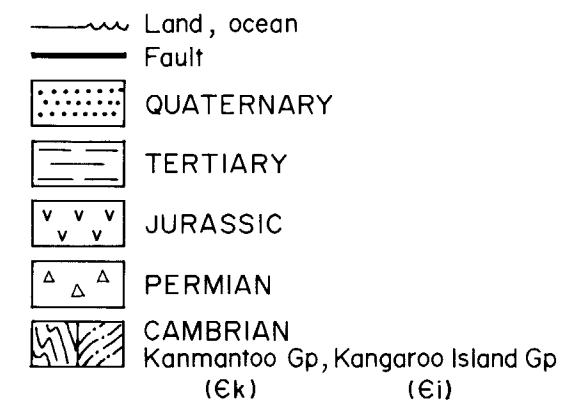
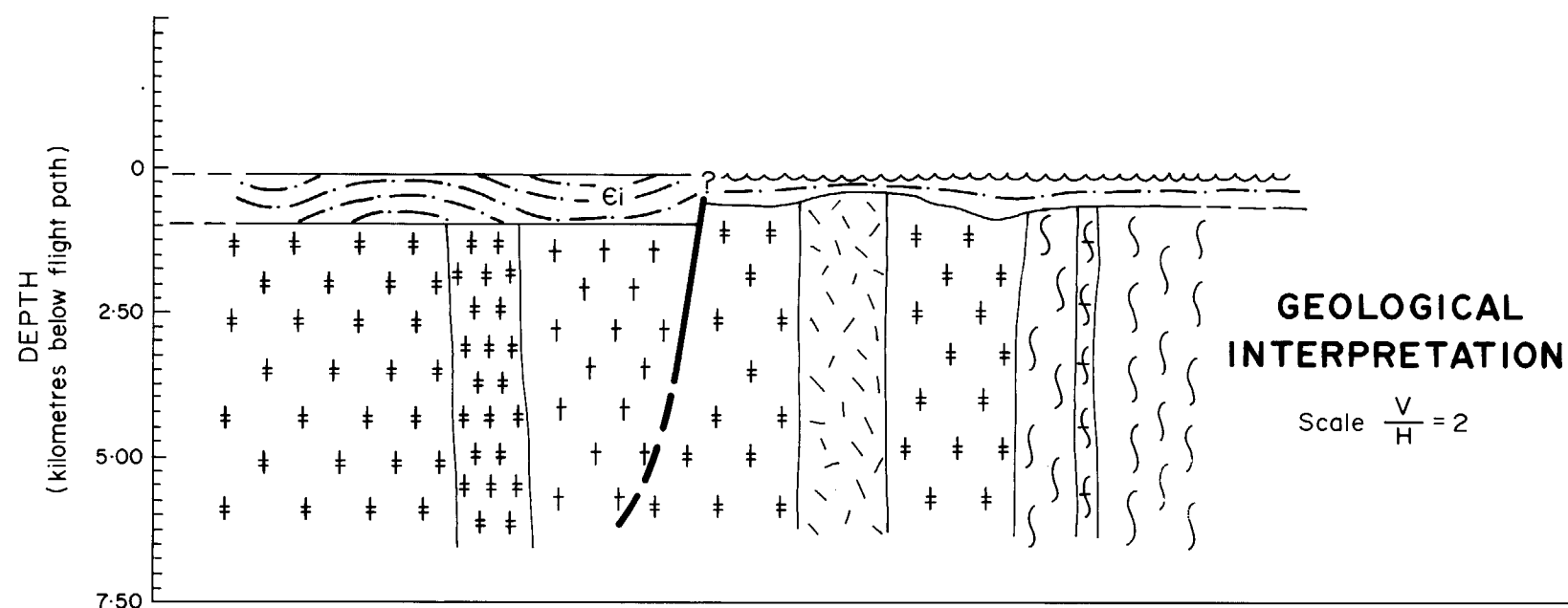
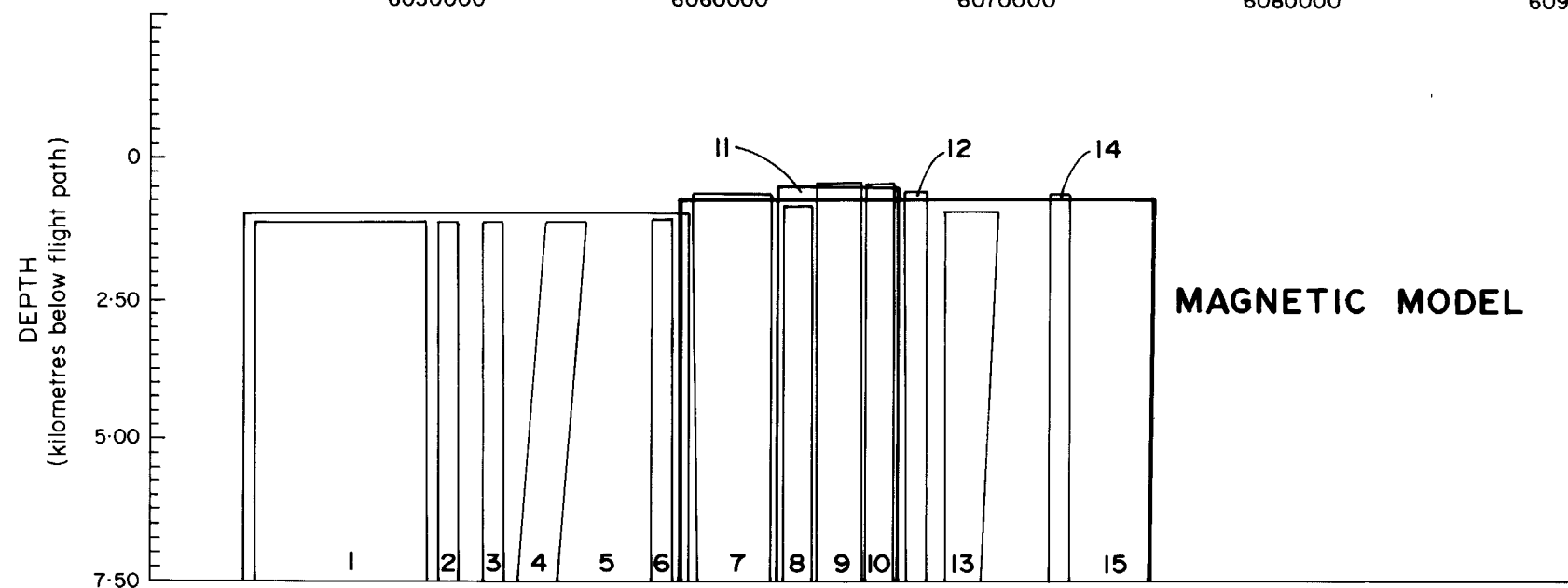
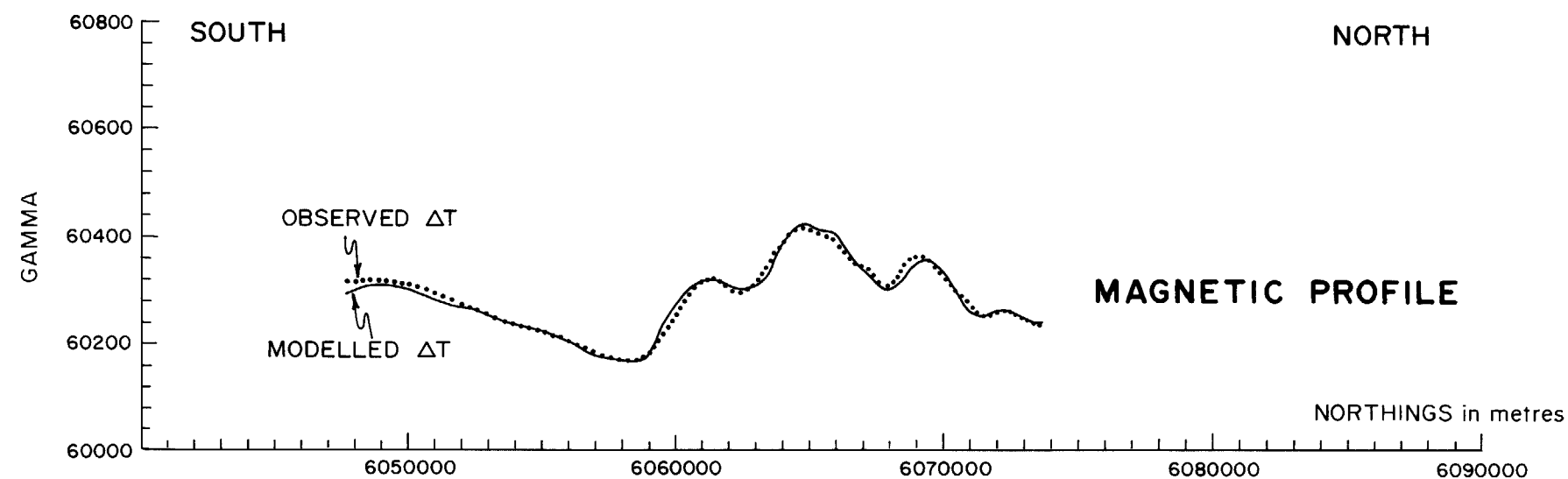


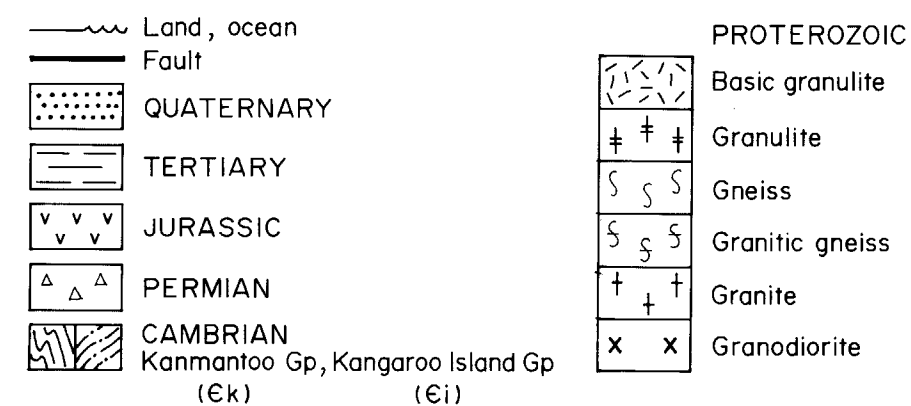
Fig. 7

## AEROMAGNETIC PROFILE MODEL AND GEOLOGICAL INTERPRETATION LINE 176 / 171



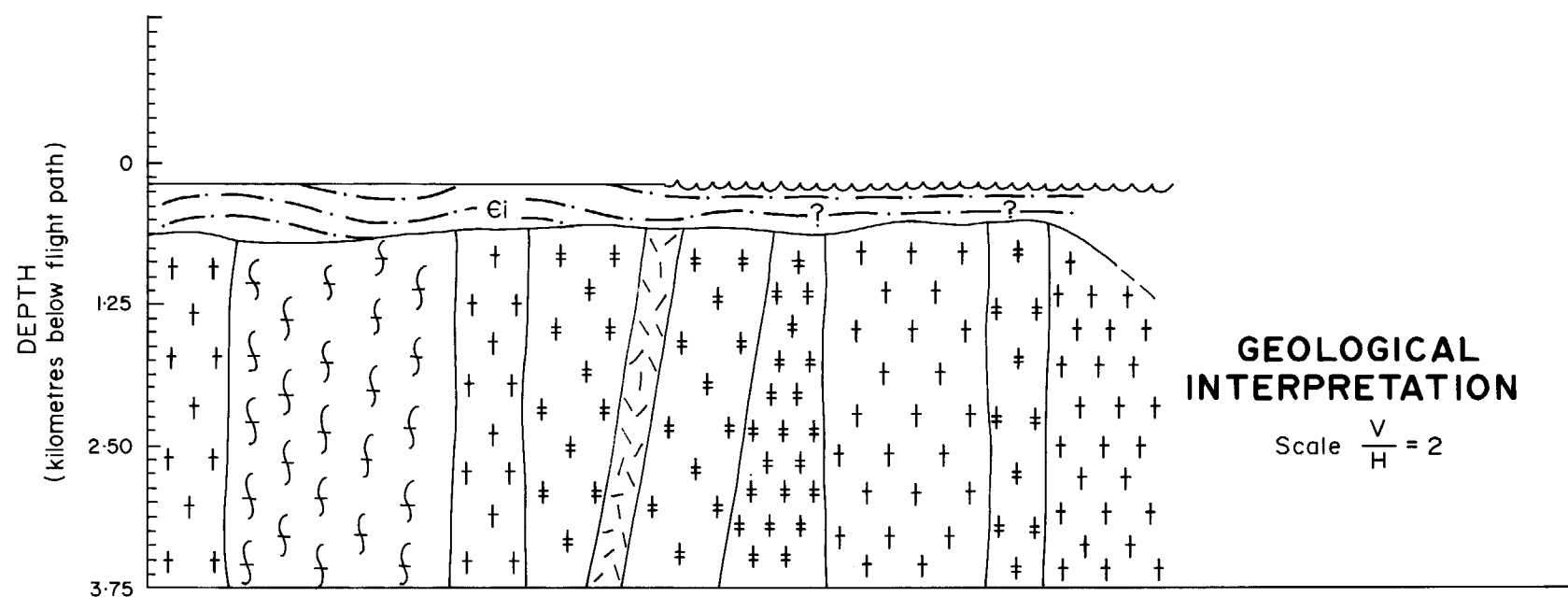
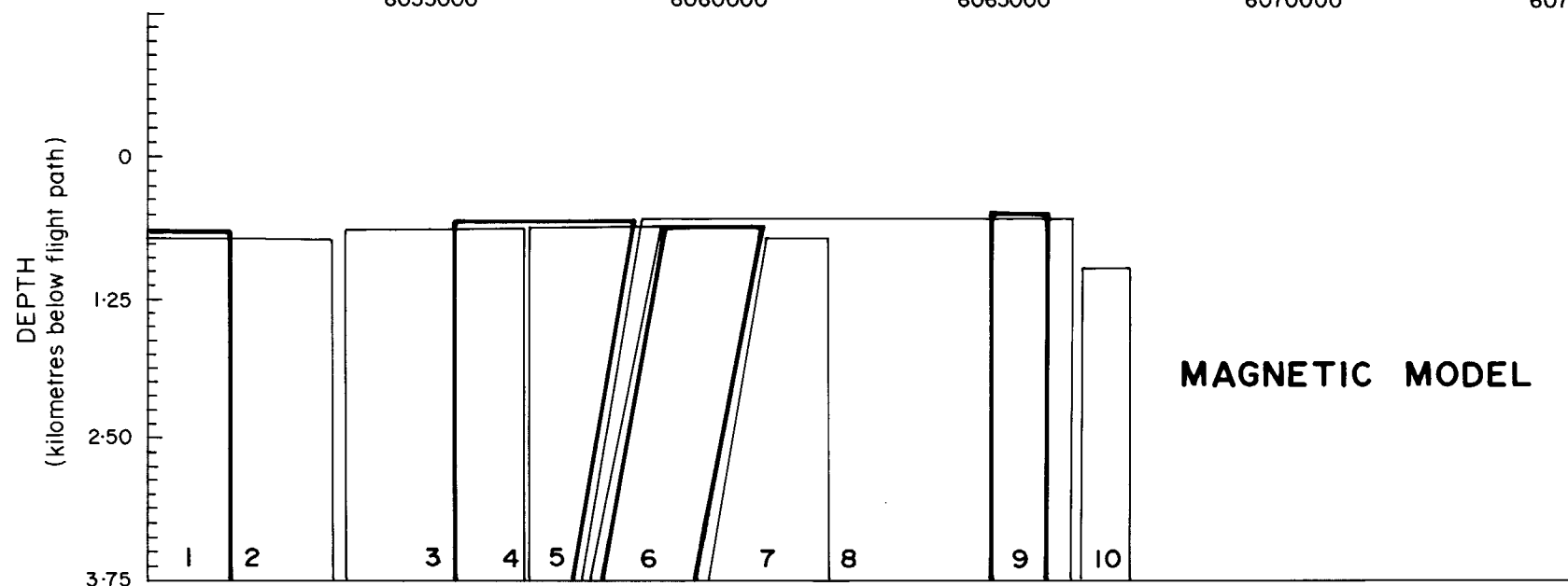
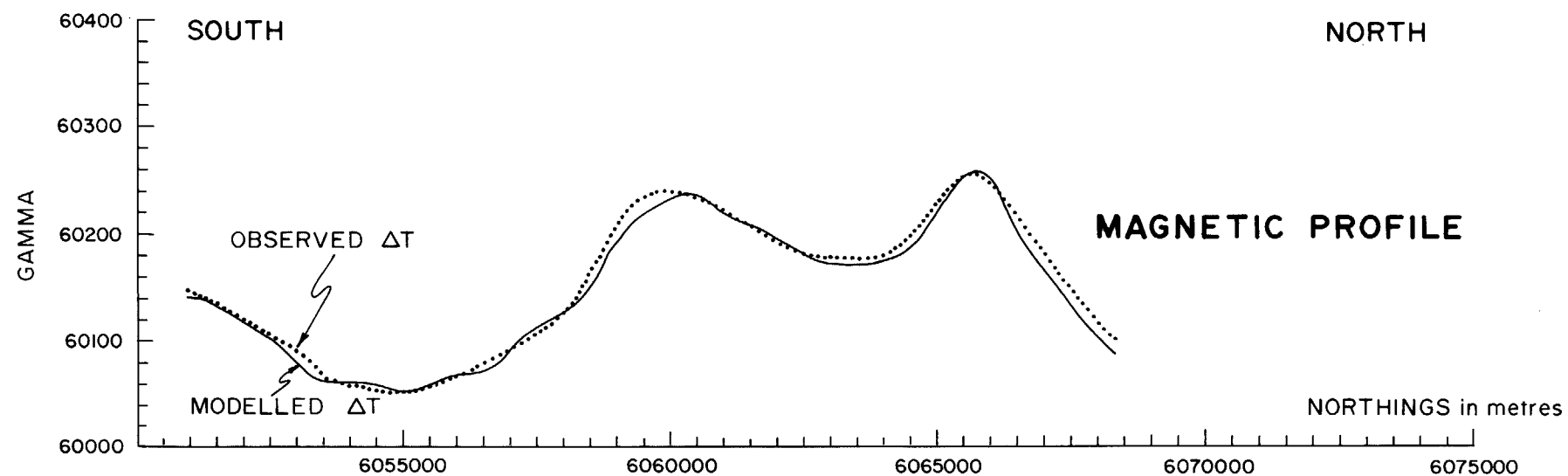
## MODEL SUMMARY

BODY No.	POSITION		DEPTH (m)	SUSCEPTIBILITY cgs units ( $\times 10^{-5}$ )
	TOP LEFT	TOP RIGHT		
1	6043744	6049745	1159	55
2	6050174	6050888	1159	40
3	6051746	6052460	1159	50
4	6053960	6055389	1159	20
5	6043315	6058961	1025	85
6	6057675	6058390	1115	50
7	6059104	6061890	669	110
8	6062319	6063319	892	80
9	6063463	6065034	491	70
10	6065177	6066177	491	45
11	6062105	6066320	535	45
12	6066534	6067320	625	70
13	6067963	6069820	981	110
14	6071606	6072321	669	40
15	6058675	6075250	758	35



**AEROMAGNETIC PROFILE  
MODEL AND GEOLOGICAL INTERPRETATION  
LINE 9170**

Fig. 8



## MODEL A SUMMARY

BODY No.	POSITION		DEPTH (m)	SUSCEPTIBILITY cgs units (x10 <sup>-5</sup> )
	TOP LEFT	TOP RIGHT		
1	6047429	6051447	646	20
2	6047004	6053233	713	70
3	6053456	6056582	624	70
4	6055377	6058502	557	25
5	6056671	6058973	600	95
6	6059042	6060738	579	60
7	6060818	6061890	702	30
8	6058636	6066182	535	85
9	6064753	6065736	490	20
10	6066347	6067180	962	80

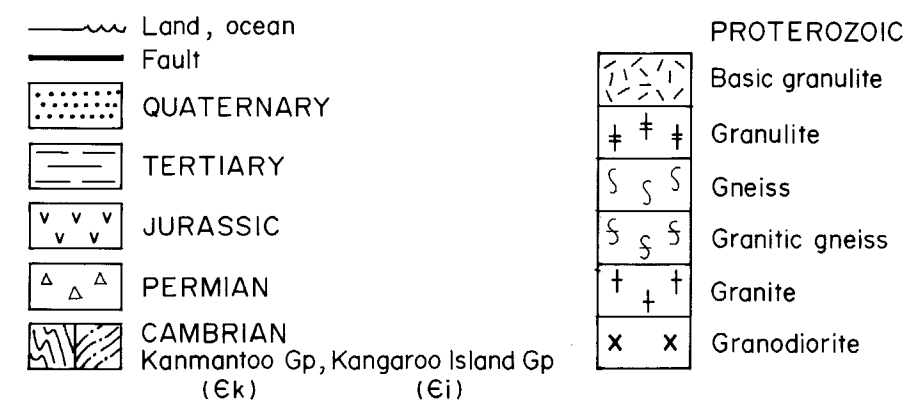
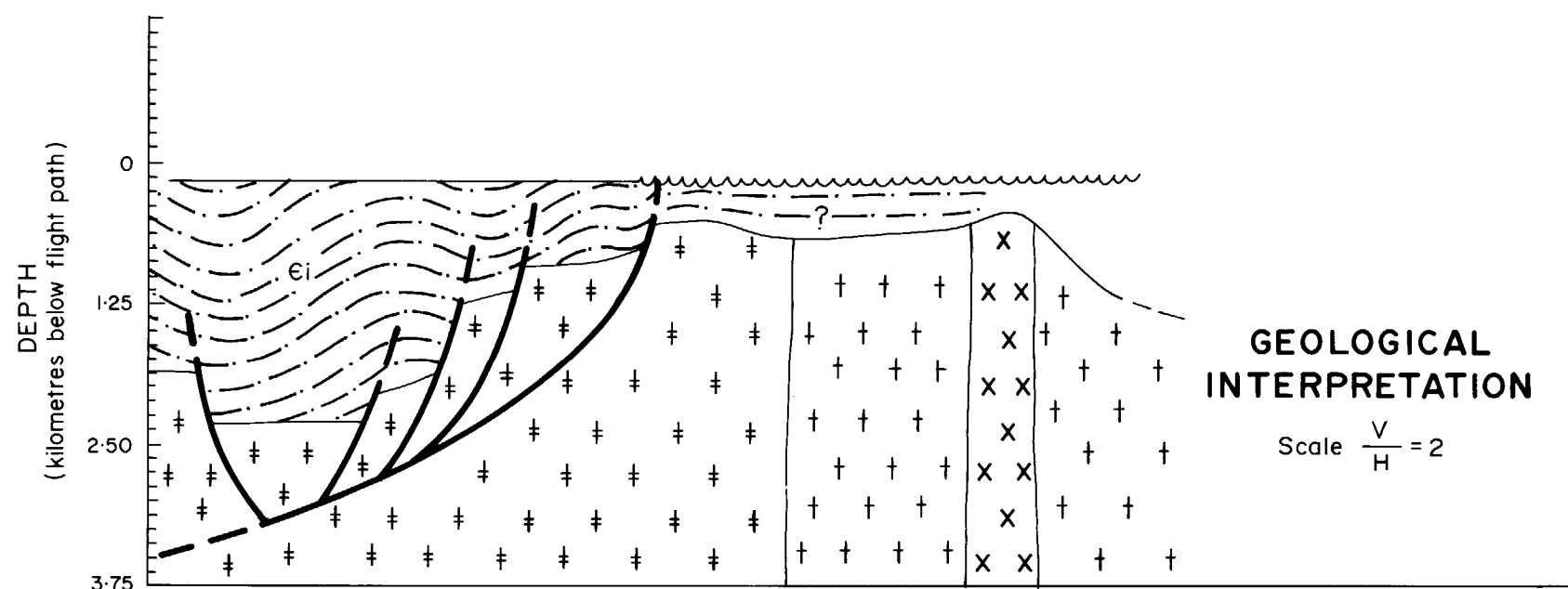
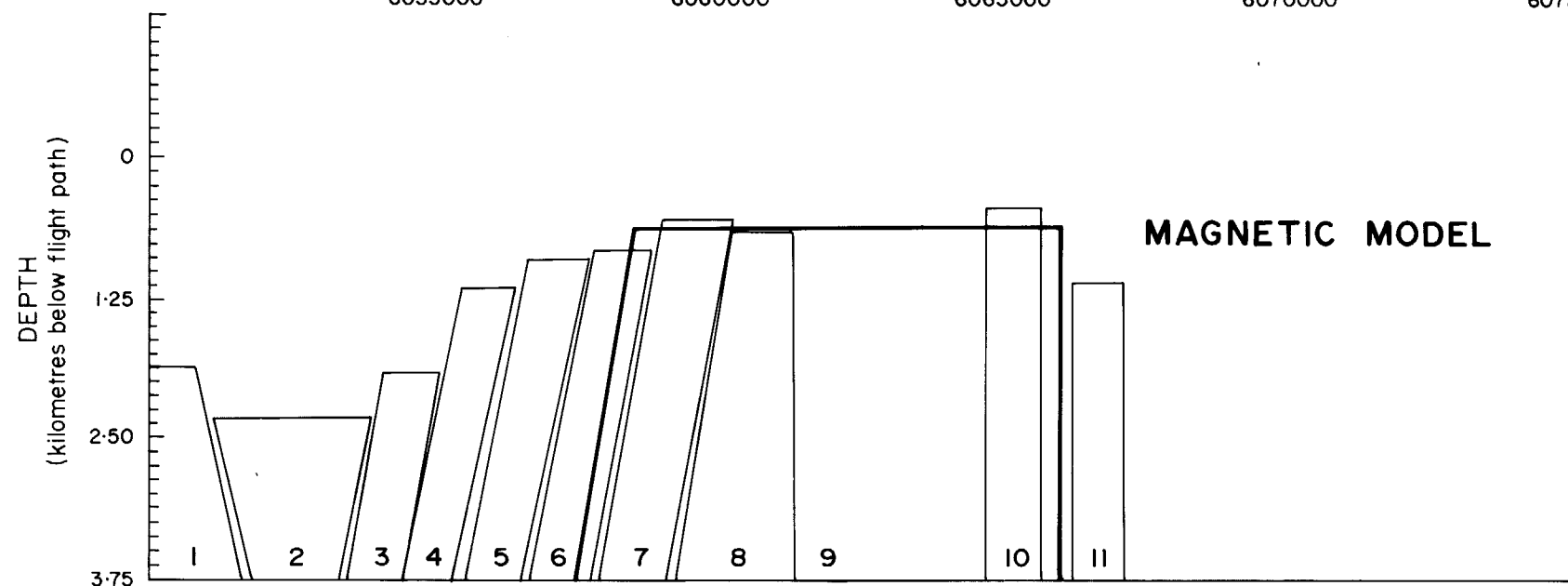
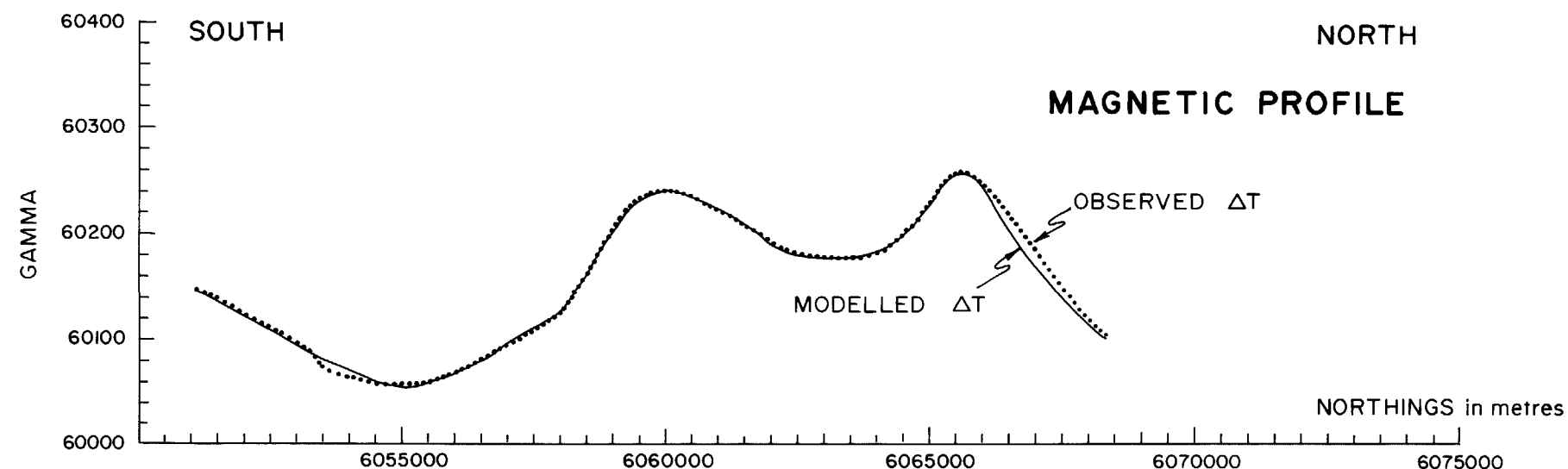


Fig. 9  
AEROMAGNETIC PROFILE  
MODEL A AND GEOLOGICAL INTERPRETATION  
LINE 9141



# MODEL B SUMMARY

BODY No.	POSITION		DEPTH (m)	SUSCEPTIBILITY cgs units (x10 <sup>-5</sup> )
	TOP LEFT	TOP RIGHT		
1	6046804	6050822	1866	150
2	6051135	6053903	2311	130
3	6054126	6055109	1922	130
4	6055511	6056448	1198	130
5	6056671	6057743	947	130
6	6057832	6058859	864	130
7	6059038	6060288	588	52
8	6060288	6061360	702	35
9	6058547	6066093	669	90
10	6064753	6065736	502	18
11	6066272	6067165	1170	80

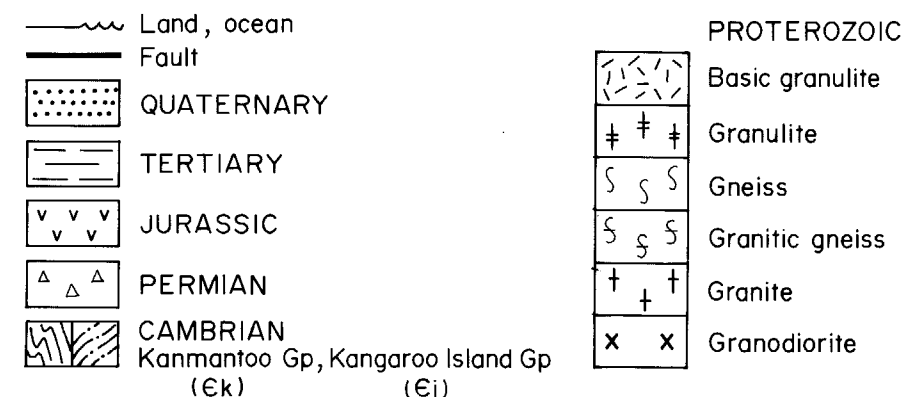
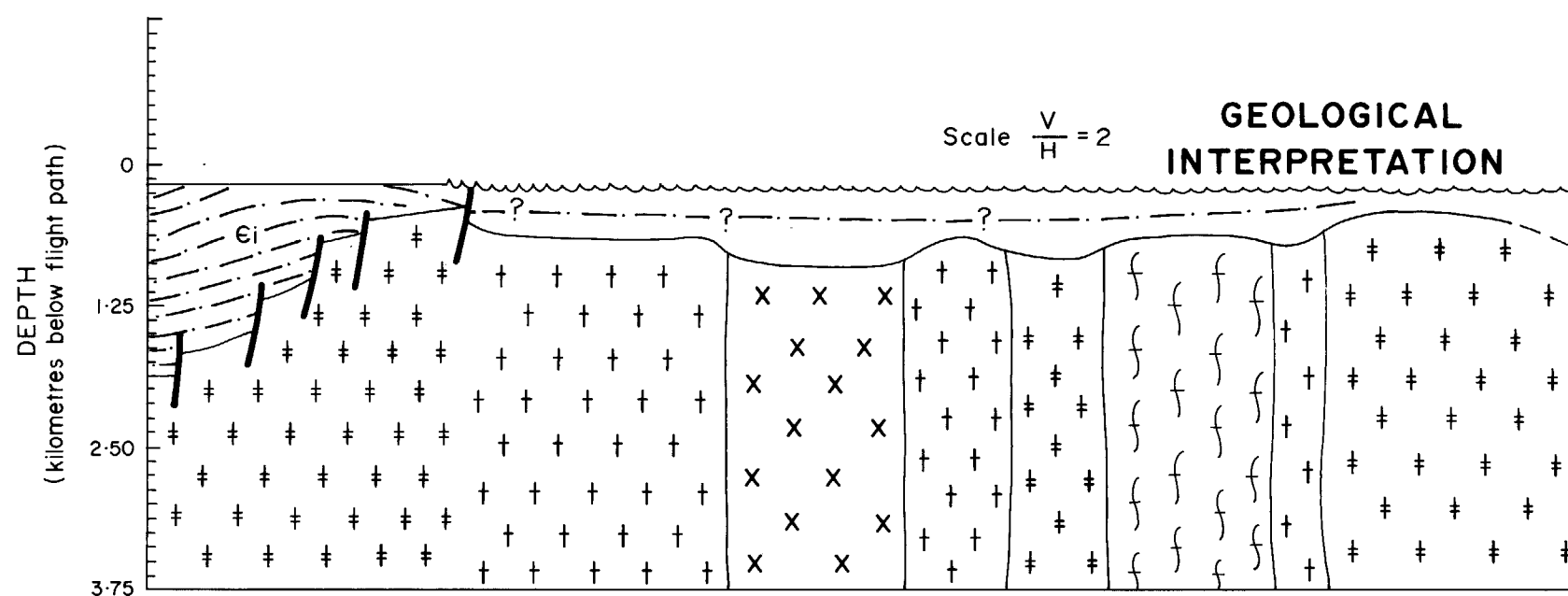
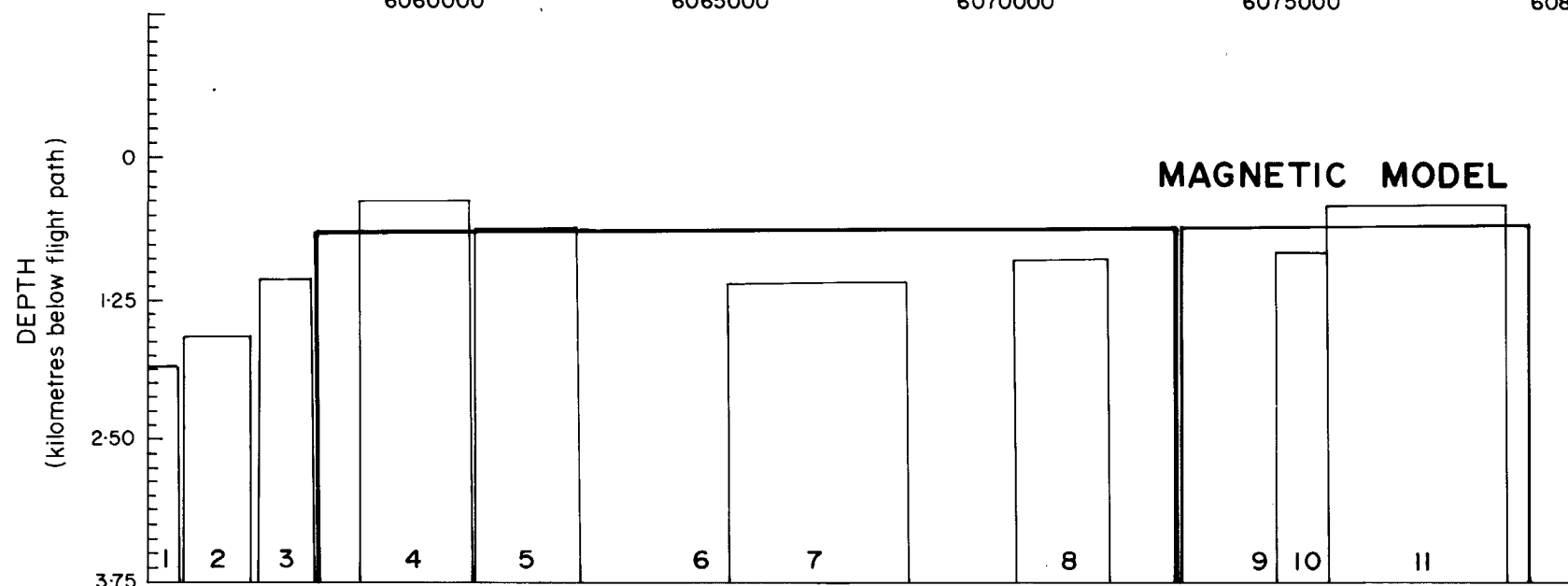
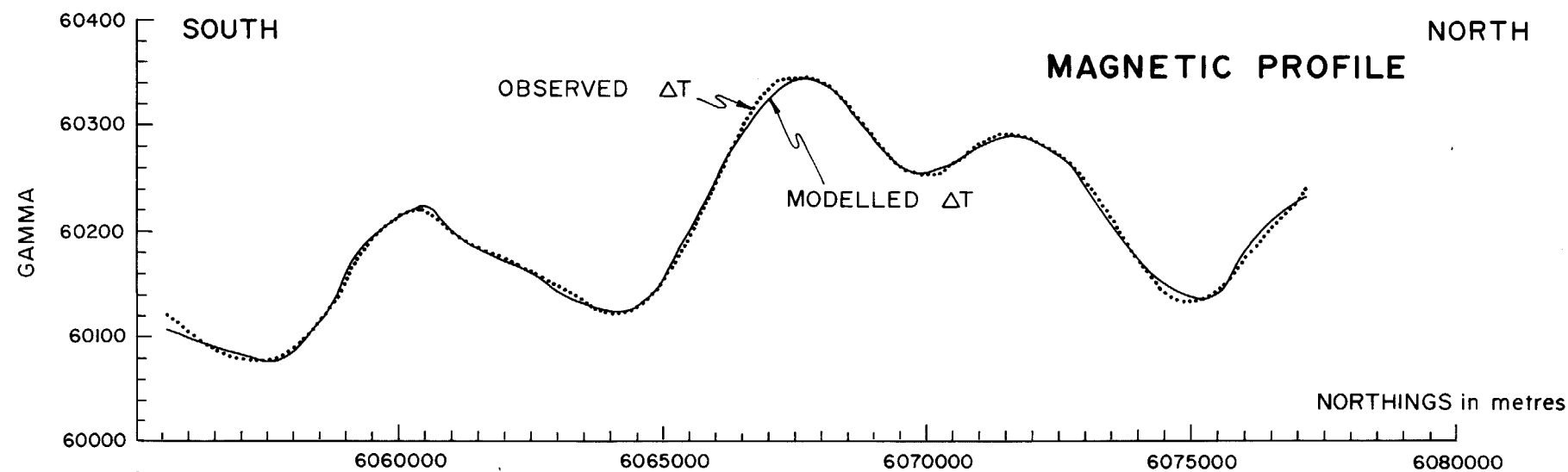


Fig. 10  
AEROMAGNETIC PROFILE  
MODEL B AND GEOLOGICAL INTERPRETATION  
LINE 9141



## MODEL SUMMARY

BODY No.	POSITION		DEPTH (m)	SUSCEPTIBILITY cgs units ( $\times 10^{-5}$ )
	TOP LEFT	TOP RIGHT		
1	6052875	6055554	1838	145
2	6055644	6056805	1588	90
3	6056983	6057876	1086	90
4	6057965	6073013	669	85
5	6058769	6060689	390	32
6	6060779	6062565	641	13
7	6065154	6068280	1142	115
8	6070155	6071807	947	40
9	6073102	6079174	669	75
10	6074754	6075647	892	17
11	6075647	6078773	479	45

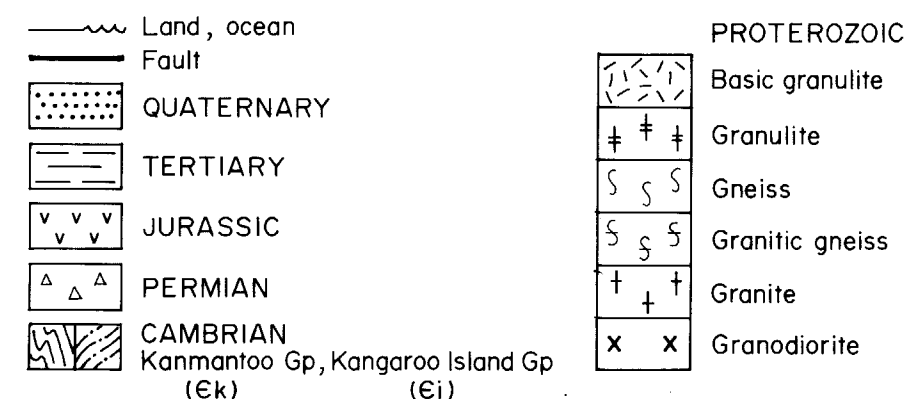
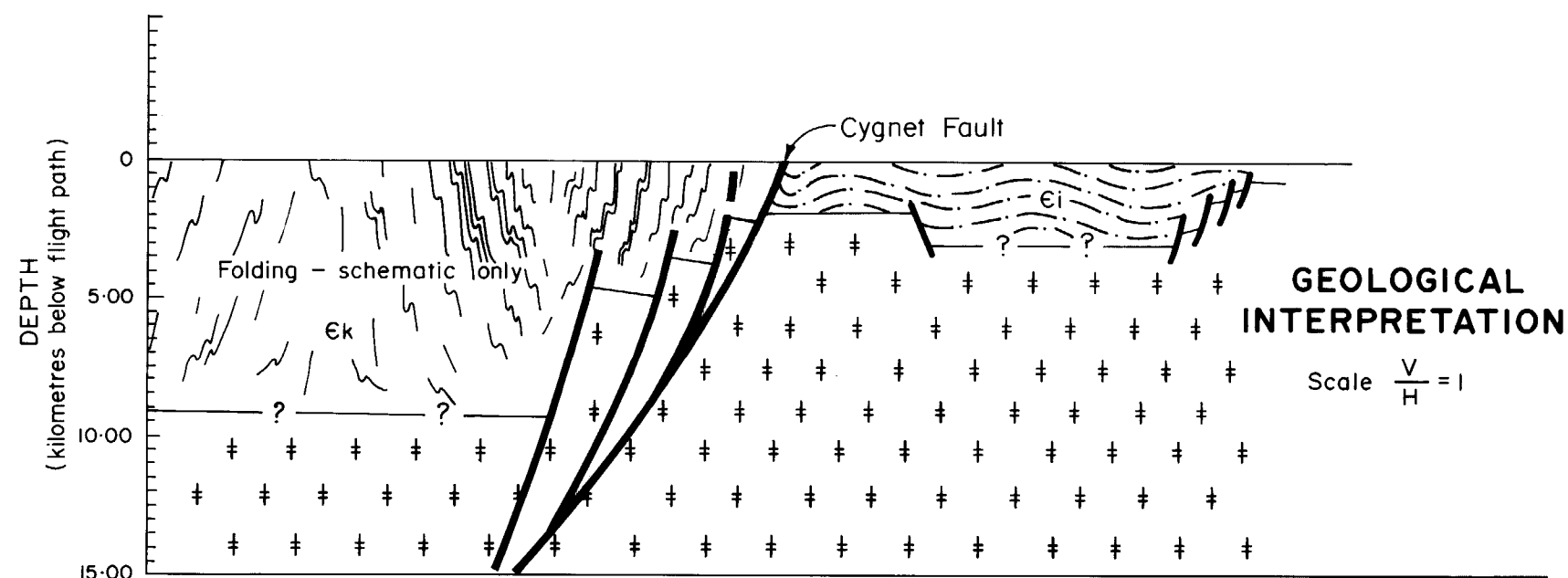
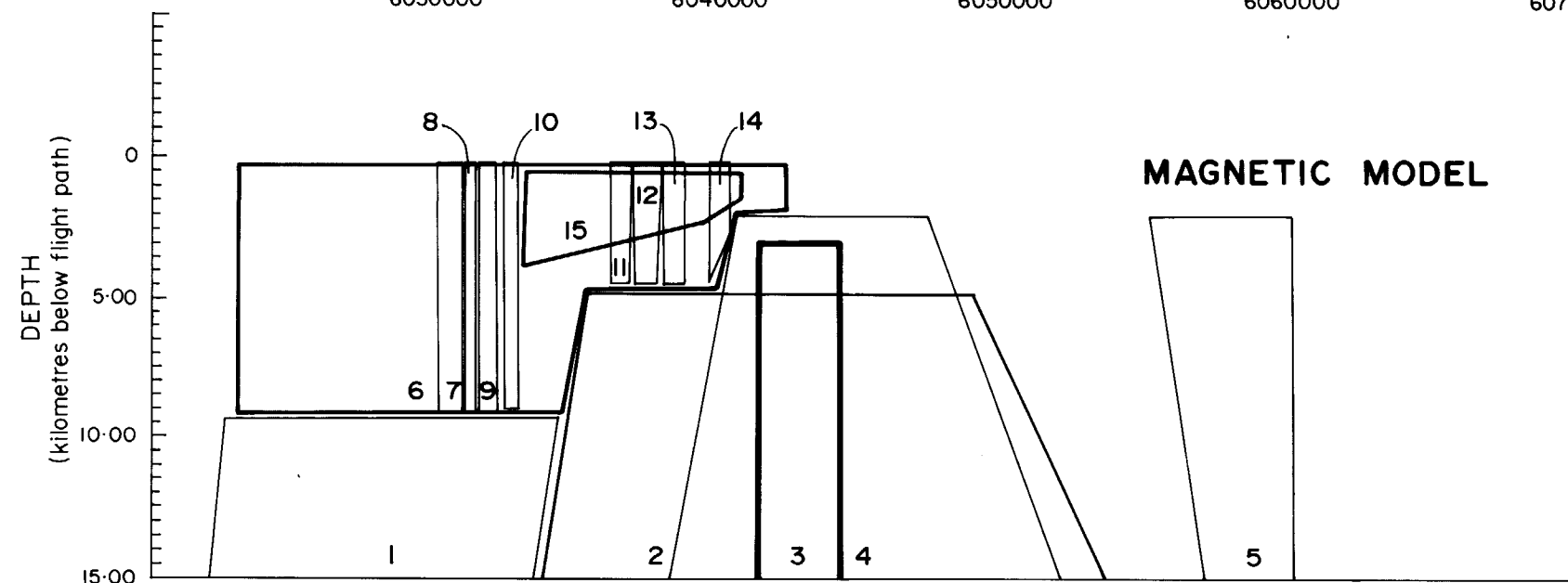
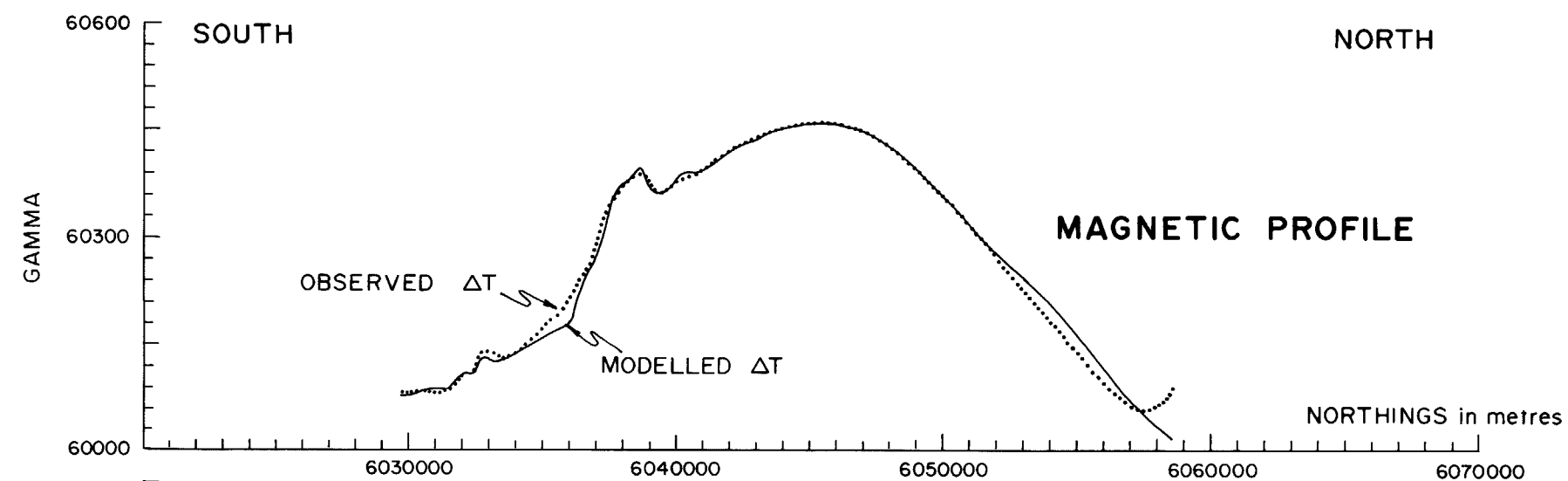


Fig. 11

**AEROMAGNETIC PROFILE  
MODEL AND GEOLOGICAL INTERPRETATION  
LINE 9120**



## MODEL SUMMARY

BODY No.	POSITION		DEPTH (m)	SUSCEPTIBILITY cgs units ( $\times 10^{-5}$ )
	TOP LEFT	TOP RIGHT		
1	6022600	6034317	9267	250
2	6035317	6048891	4813	480
3	6041390	6044247	3031	60
4	6040603	6047319	2051	25
5	6055106	6060107	2051	60
6	6023029	6042318	269	5
7	6030102	6030959	180	4
8	6031030	6031388	218	5
9	6031530	6032173	168	10
10	6032388	6032888	224	18
11	6036174	6036889	168	19
12	6036960	6037960	180	36
13	6037960	6038746	180	26
14	6039603	6040318	179	5
15	6033174	6040747	536	10

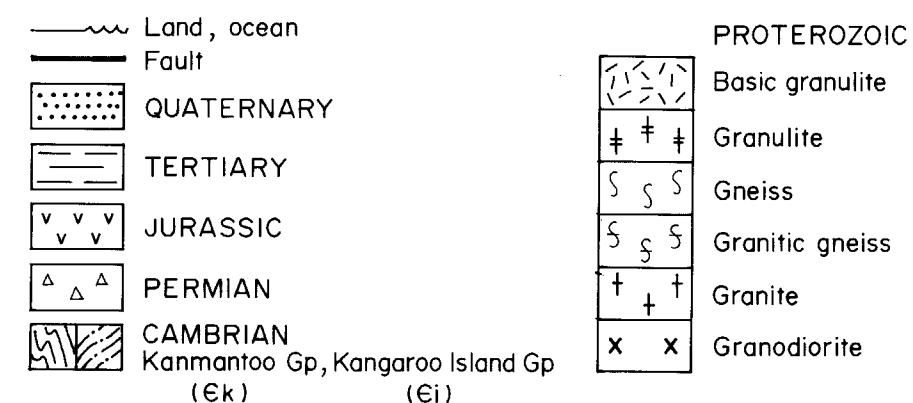
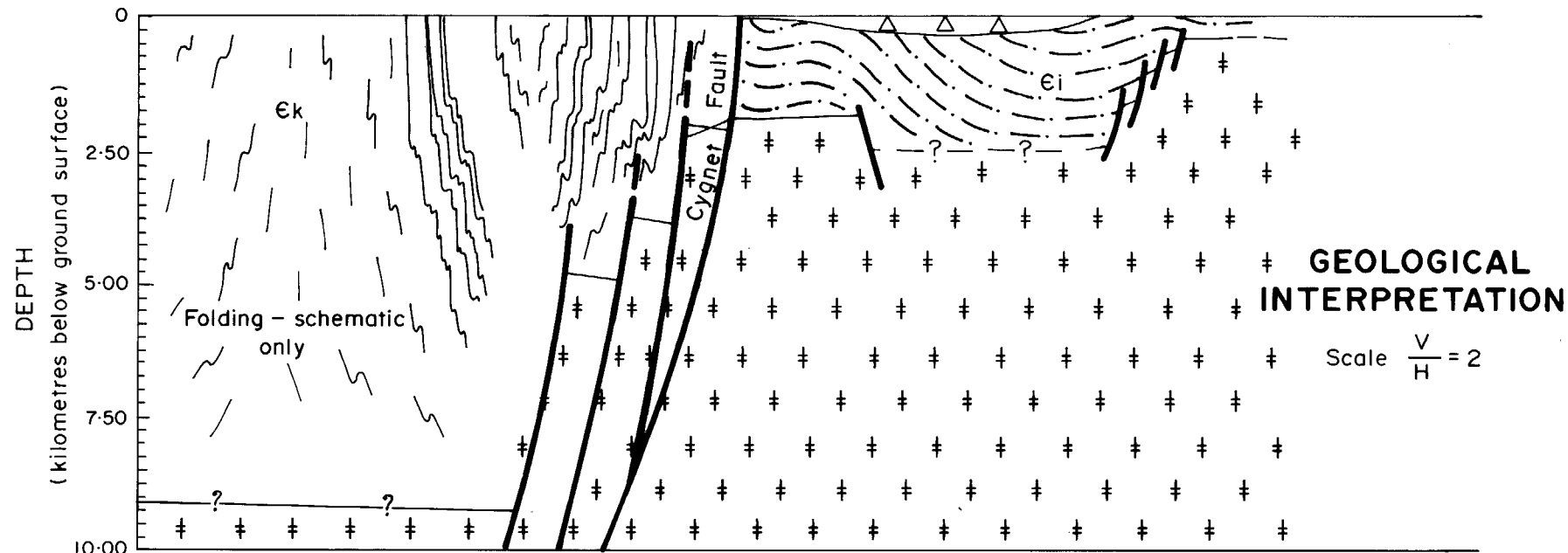
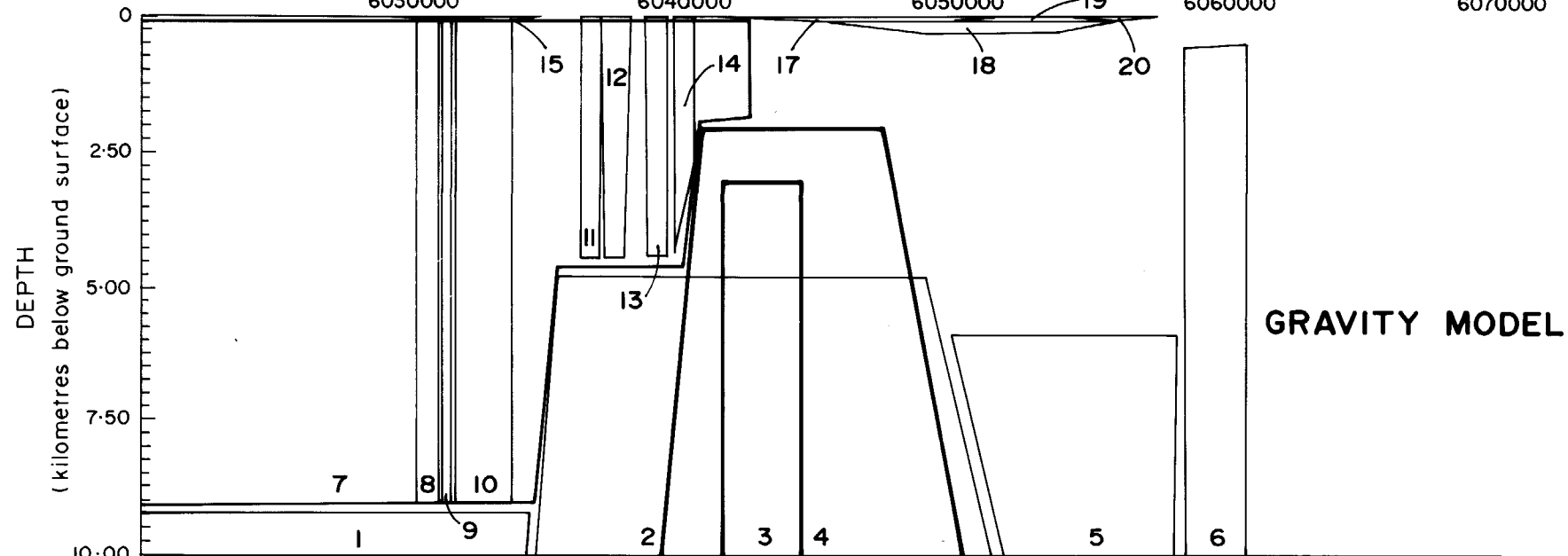
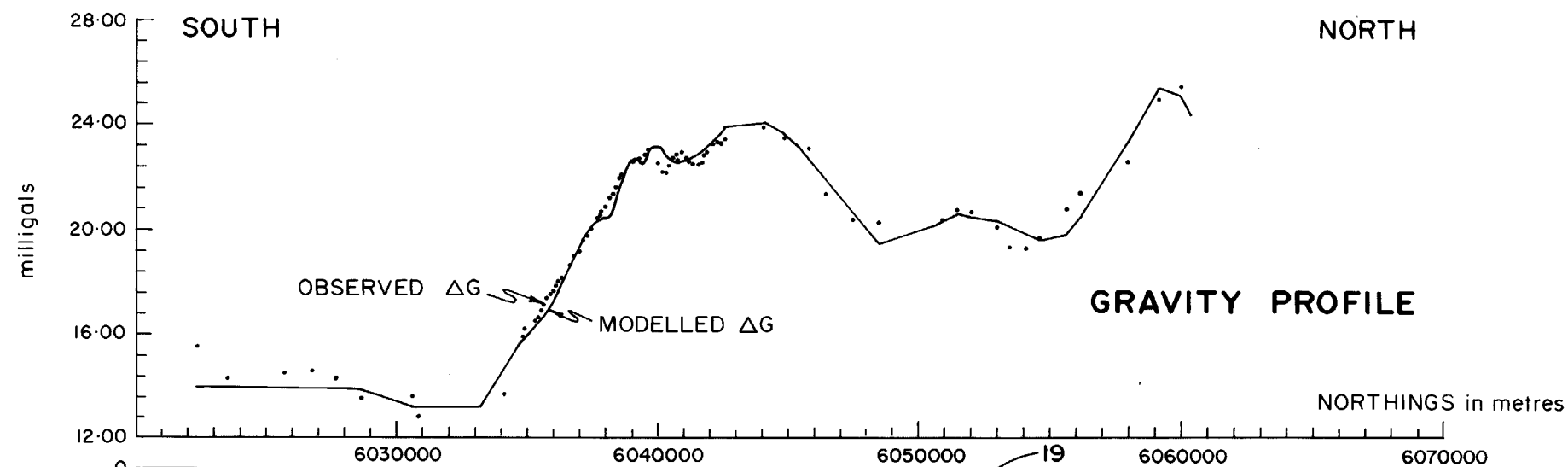


Fig. 12  
AEROMAGNETIC PROFILE  
MODEL AND GEOLOGICAL INTERPRETATION  
LINE 9122



# MODEL SUMMARY

BODY No.	POSITION		DEPTH (m)	DENSITY CONTRAST (g/cc)
	TOP LEFT	TOP RIGHT		
1	6014449	6034317	9256	0.140
2	6035317	6048891	4813	0.040
3	6041390	6044247	3031	0.100
4	6040603	6047319	2051	0.130
5	6049863	6058079	5904	0.130
6	6058347	6060643	~551	0.140
7	6014187	6042362	91	-0.025
8	6030127	6030931	45	-0.020
9	6031020	6031378	58	0.010
10	6031556	6033610	65	-0.025
11	6036200	6036914	7	0.025
12	6036914	6037986	7	0.050
13	6038522	6039326	7	0.085
14	6039593	6040308	5	0.075
15	6023162	6034592	2	-0.250
16	6040040	6059508	2	-0.250
17	6040219	6051024	~19	-0.200
18	6053346	6058793	13	-0.200
19	6051203	6053078	9	0.700
20	6044594	6055846	88	-0.220

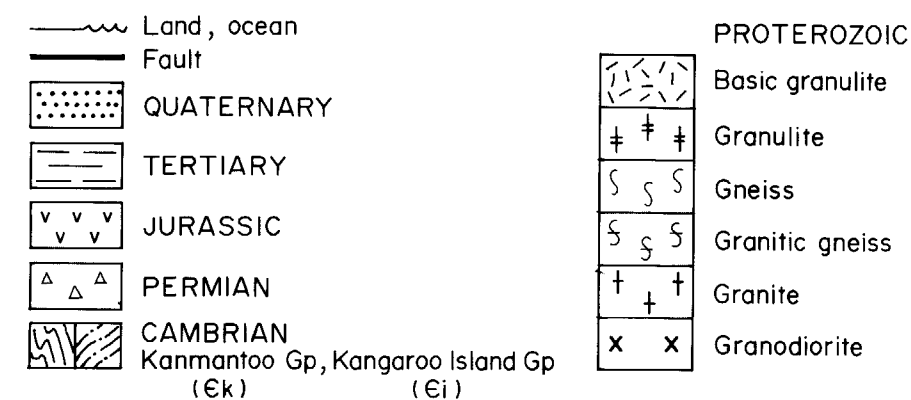
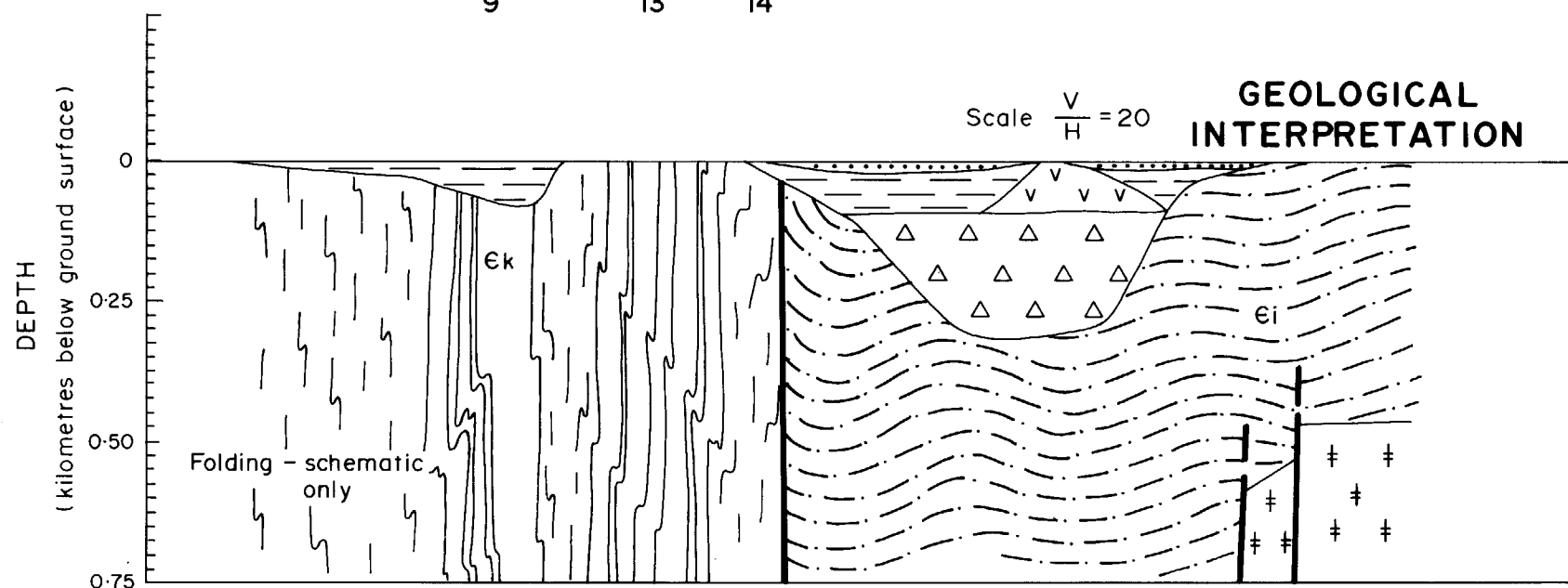
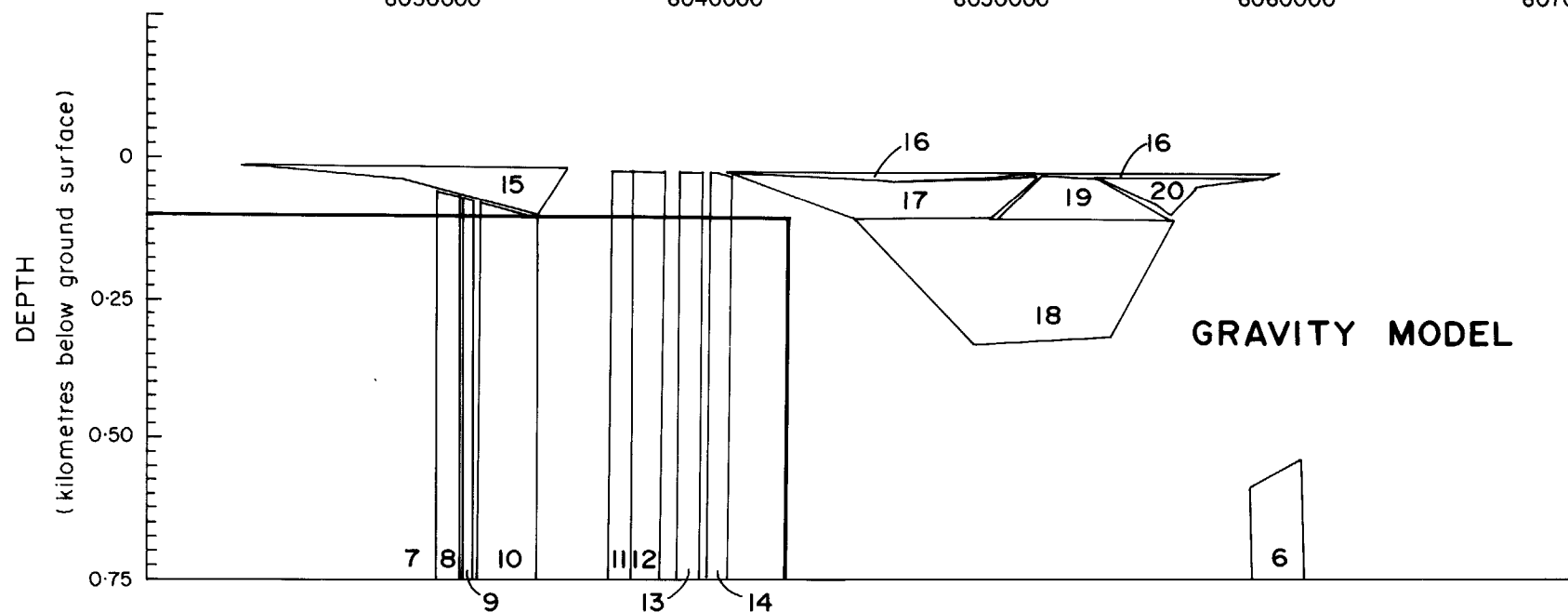
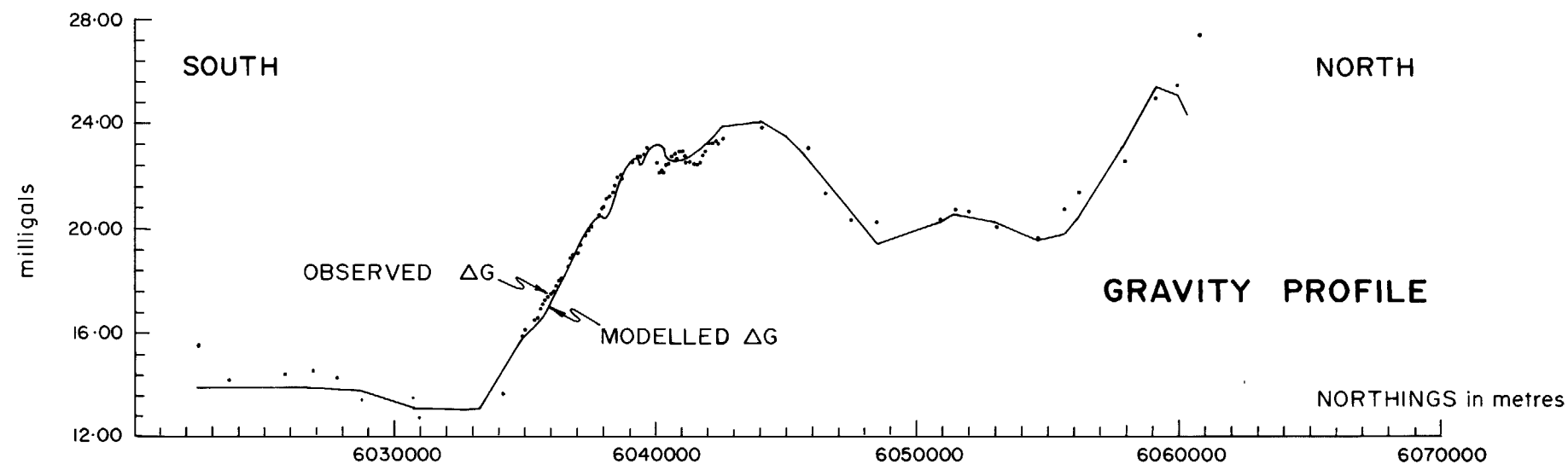


Fig. 13

**GRAVITY PROFILE  
MODEL AND GEOLOGICAL INTERPRETATION  
LINE 3A**



## MODEL SUMMARY

BODY No.	POSITION		DEPTH (m)	DENSITY CONTRAST (g/cc)
	TOP LEFT	TOP RIGHT		
1	6014449	6034317	9256	0.140
2	6035317	6048891	4813	0.040
3	6041390	6044247	3031	0.100
4	6040603	6047319	2051	0.130
5	6049863	6058079	5904	0.130
6	6058347	6060643	~551	0.140
7	6014187	6042362	91	-0.025
8	6030127	6030931	45	-0.020
9	6031020	6031378	58	0.010
10	6031556	6033610	65	-0.025
11	6036200	6036914	7	0.025
12	6036914	6037986	7	0.050
13	6038522	6039326	7	0.085
14	6039593	6040308	5	0.075
15	6023162	6034592	2	-0.250
16	6040040	6059508	2	-0.250
17	6040219	6051024	~19	-0.200
18	6053346	6058793	13	-0.200
19	6051203	6053078	9	0.700
20	6044594	6055846	88	-0.220

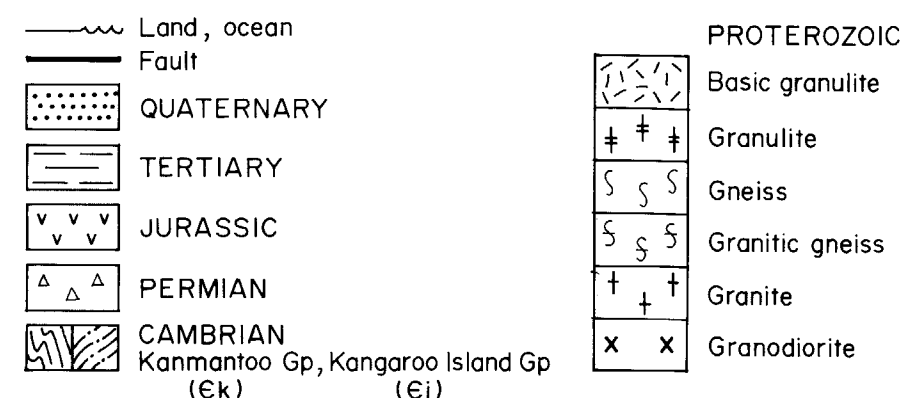
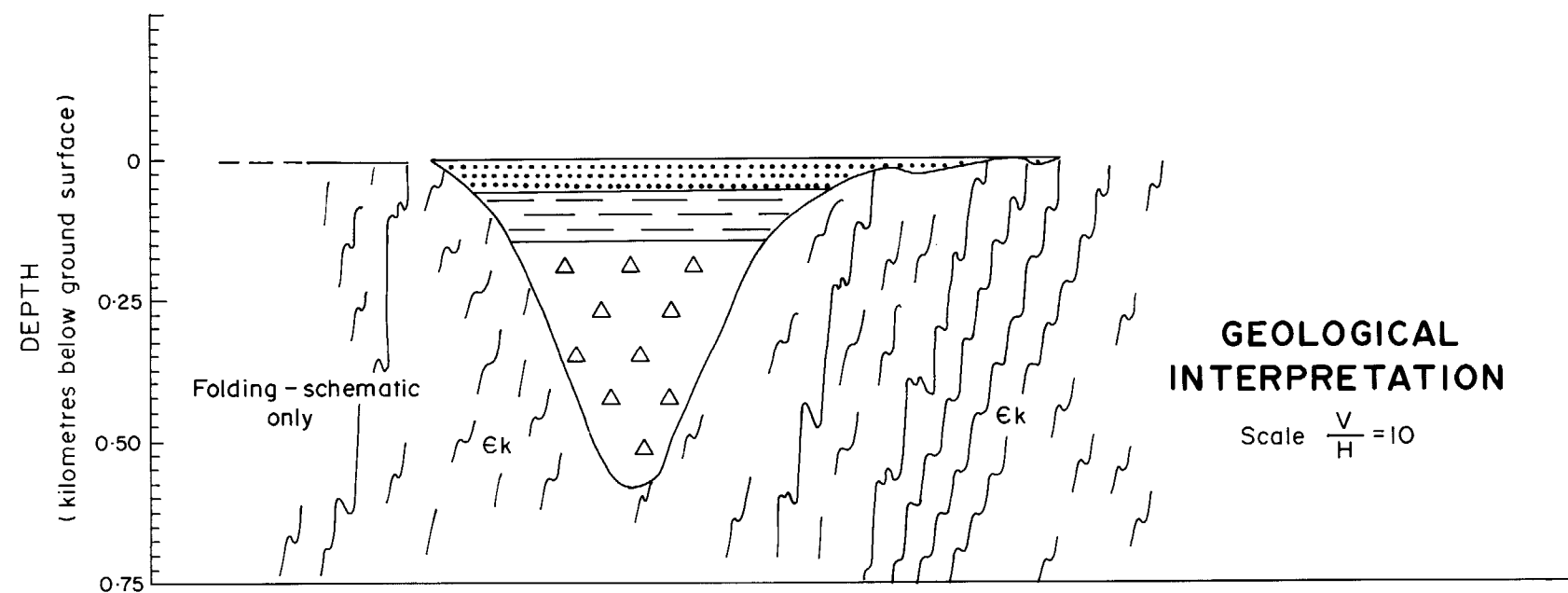
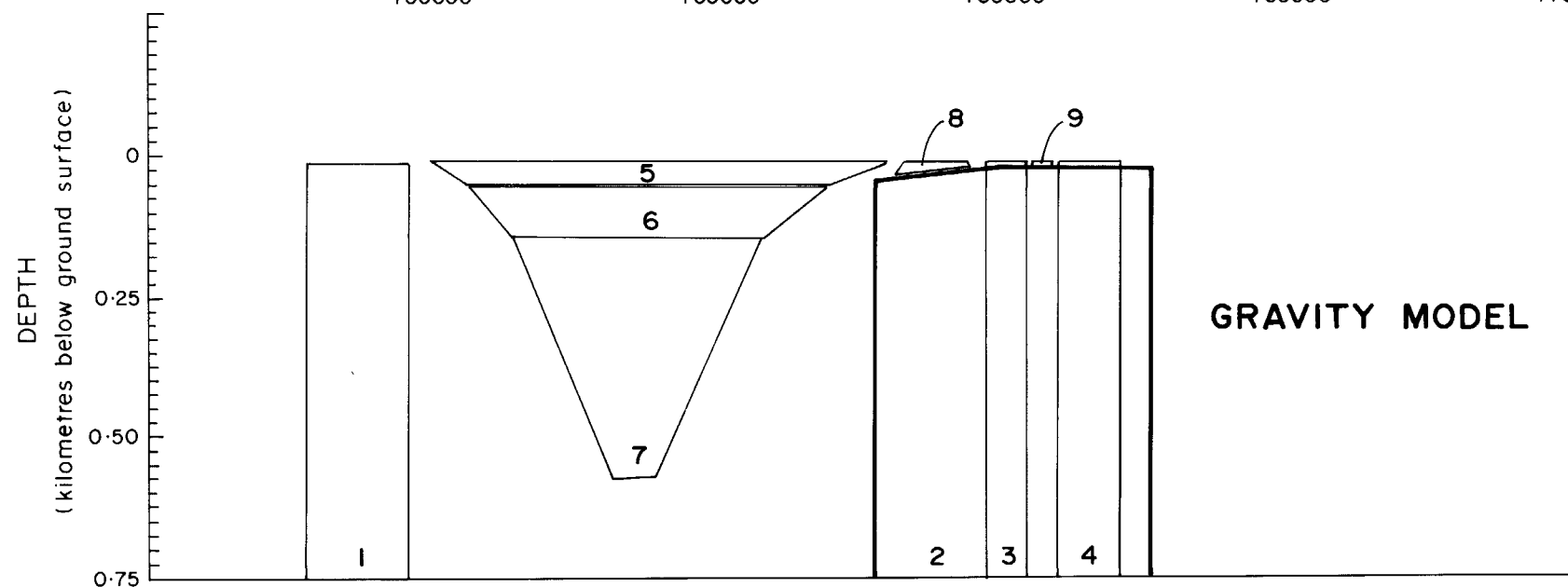
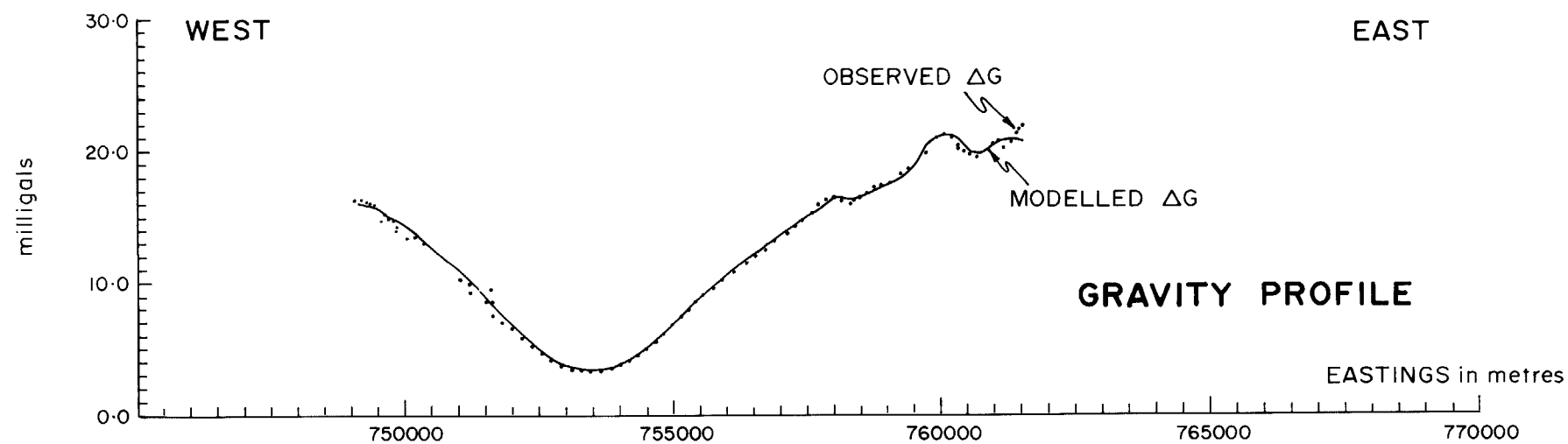


Fig. 14

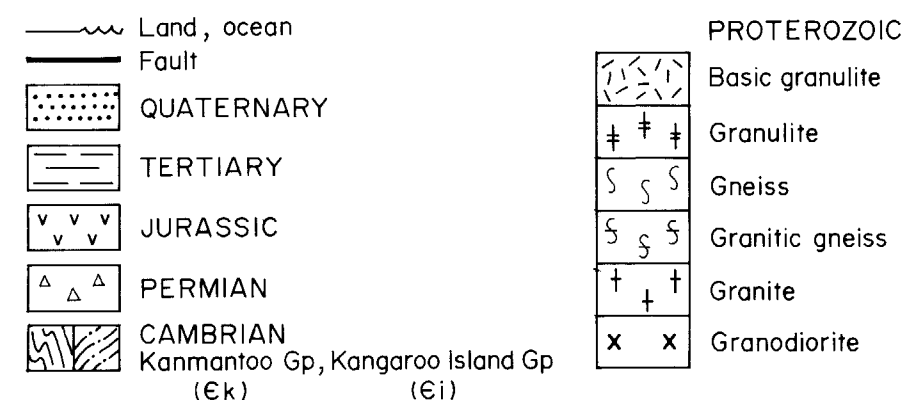
**ENLARGEMENT OF GRAVITY  
MODEL AND GEOLOGICAL INTERPRETATION  
LINE 3A**





## MODEL SUMMARY

BODY No.	POSITION		DEPTH (m)	DENSITY CONTRAST (g/cc)
	TOP LEFT	TOP RIGHT		
1	747728	749515	11	0.050
2	759874	762588	11	0.035
3	759695	760409	5	0.180
4	760981	762053	5	0.100
5	749943	757980	5	-0.780
6	750586	756873	54	-0.680
7	751336	755694	147	-0.480
8	758230	759374	5	-0.800
9	760517	760874	5	-0.780



**GRAVITY PROFILE  
MODEL AND GEOLOGICAL INTERPRETATION  
LINE 2A**

Fig. 15

